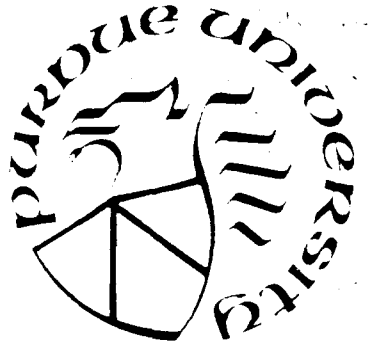

PURDUE UNIVERSITY
West Lafayette, Indiana

TURNER LABORATORY FOR ELECTROCERAMICS

(4)

METALLO-ORGANIC DECOMPOSITION PROCESS FOR DIELECTRIC FILMS

R.W. Vest and G.M. Vest

15 June 1989

Annual Report for the Period:

4/1/88 - 3/31/89

Contract No.: N00014-83-K-0321

Prepared for:

OFFICE OF NAVAL RESEARCH

TABLE OF CONTENTS

FOREWORD

The research described in this report was conducted under Contract No. N00014-83-K-0321 with the Office of Naval Research under the technical cognizance of Dr. W.A. Smith. Research was conducted in the Turner Laboratory for Electroceramics, School of Materials Engineering and School of Electrical Engineering, Purdue University, West Lafayette, Indiana under the direction of R.W. Vest and G.M. Vest. Contributing to the project were Messers. G.L. Skiles, K.D. Sutton, R.C. Wu, J. Xu and Ms. L.C. Veitch. This annual report contains results of basic research on metallo-organic systems which are applicable to all dielectric films, plus the results of studies of three particular types of films.

1. INTRODUCTION

The metallo-organic decomposition (MOC) process is a technique for producing inorganic films without processing in vacuum or going through a gel or powder step. The processing starts with metallo-organic compounds of the desired elements dissolved in an appropriate solvent. These solutions of individual metallo-organic compounds are then mixed in the appropriate ratio to give the desired cation stoichiometry for the final film to produce a formulation, which is itself a true solution. This formulation is deposited on a substrate by any of a variety of techniques to produce a wet film, which is then heated to first remove any solvent that did not evaporate during the deposition step and then to decompose the metallo-organic compounds to produce an inorganic film. A significant volume change occurs in going from the wet film to the inorganic film; if the inorganic film produced by a single pass through the process is not as thick as desired, the deposition and pyrolysis steps can be repeated as many times as necessary to produce a multilayer film of the required thickness. After the desired film thickness is achieved, the films are often subjected to a further heat treatment to control features such as oxygen stoichiometry, grain size or preferred orientation.

The advantages and limitations of the MOD process were discussed in the previous annual report [1]. Also covered in the previous report was some of our basic research on metallo-organic systems, including selection and synthesis of compounds and solvent considerations. This report covers some basic research on MOD processing, including studies of film deposition, pyrolysis and annealing, and also discusses results obtained for MOD films of PZT, PMN, PNN, PFN and $LiNbO_3$.

2. MOD FILM PROCESSING

2.1 Film Deposition

In principle, the formulation solution can have any desired viscosity and surface tension by use of appropriate solvents and additives, which means that any technique that has ever been used to deposit a liquid on a solid surface can be used to deposit the formulation solution on the substrate. A number of printing methods for patterning during the deposition step can be used, but the primary interest for the dielectric films of concern for this project are methods of depositing a uniform film over the entire substrate. Several of the advantages of MOD processing require that the formulation deposited on the substrate be a true solution, so the deposition method must not cause any segregation of the metallo-organic compounds. Regardless of the solvent system used, the different metallo-organic compounds in a given formulation solution will have different solubilities, so if there is any evaporation during the deposition step it should be very rapid so as to minimize segregation. A desirable feature of any deposition method is the ability to control both the magnitude and uniformity of film thickness because many physical and structural properties of MOD films are related to the single layer thickness.

The methods that have been used to deposit a uniform coating of the formulation solution on a substrate are generally those which have been developed for depositing photoresist in the microelectronics industry and include spinning, dipping or spraying techniques. Dipping with a controlled rate of withdrawl is the deposition method recommended by Nippon Soda* for depositing solutions of their metallo-organic compounds of Si, Ti, In, Zr and Ta. They

---

* Nippon Soda Co., Ltd., Shin Ohtemachi Bldg., 2-2-1 Ohtemachi, Chiyoda-ku, Tokyo, Japan.

recommend deposition by submerging the substrate in the metallo-organic formulation and then withdrawing at speeds from 10-40 cm/min. For example, in their trade literature they show that starting with a formulation solution that will produce 8 wt.% SiO_2, the fired film thickness can be varied from 150 to 250 nm by varying the withdrawl speed from 10 to 40 cm/min.

By far the most common technique that has been used to deposit a uniform film of the formulation solution on a substrate has been spin coating. The substrate is placed on a turntable and a premeasured amount of formulation solution is dispensed onto the substrate. The spinning is initially done at a slow rate to assure complete coverage of the substrate, and this is then followed by fast spinning for a longer duration. In order to avoid dust streaks in the film the spinning should be carried out in a clean environment, preferable class 100 or better. A fluid dynamics analysis of the spin coating process derived from the Navier-Stokes equation in cylindrical coordinates was reported [2] for a simple system of a nonvolatile Newtonian fluid, and included the contribution of interface slip between the liquid film and the rotating disk. This approach resulted in the following equation for the time rate of change of film thickness h:

$$\frac{dh}{dt} = \frac{-2\rho_l \omega^2 h^2}{3\eta} (h+3\lambda) \qquad (1)$$

where ρ_l is the liquid density, ω is the angular velocity, η is the viscosity of the liquid and λ is the slip coefficient. The second term in Eq. 1, which represents an increased flow due to interfacial slip, is generally negligible because the slip coefficient is very small for most liquid-solid couples. If the slip term is neglected, Eq. 1 can be integrated to give:

$$h = \frac{h_o}{(1+4\rho_l \omega^2 h_o^2 t/3\eta)^{1/2}} \qquad (2)$$

where h_o is the liquid film thickness at $t = 0$, which represents the time at which fast spinning is initiated. Some typical values for spin coating of formulation solutions are:

$\rho_l = 1$ g/cm^3

$\eta = 10$ mPa·s

$\omega = 7.5 \times 10^5$ radians/s (2000 rpm)

$h_o = 6$ μm

$t = 30$ s

Using these values, the second term in the denominator in Eq. 2 is 8.2×10^7, which is certainly much greater than 1, and Eq. 2 reduces to

$$h = \frac{1}{2\omega}\left(\frac{3\eta}{\rho_l t}\right)^{1/2} \tag{3}$$

One consequence of Eq. 3 is that the final liquid film thickness is independent of the initial film thickness or the amount of formulation solution transferred to the substrate. The thickness of the solid film after pyrolysis (h_s) can be calculated from:

$$h_s = h\,\frac{\rho_l}{\rho_s} C \tag{4}$$

where ρ_s is the density of the solid film and C is the concentration of the formulation solution (g solid film/g solution). Combining Eqs. 3 and 4 gives

$$h_s = \frac{C}{2\omega\rho_s}\left(\frac{3\eta\rho_l}{t}\right)^{1/2} \tag{5}$$

An equimolar formulation solution of lead neodecanoate and titanium di-methoxy-di-neodecanoate in xylene solvent was used to collect experimental data [3] to compare with Eq. 5. The thicknesses of the fired $PbTiO_3$ films were determined for various formulation solution concentrations and viscosities, and for the spinning parameters of speed and time. Figure 1a shows the experimental and calculated fired film thickness as a function of spinning speed at fixed spinning time and solution viscosity. At the lower spinning speed the calculated thickness

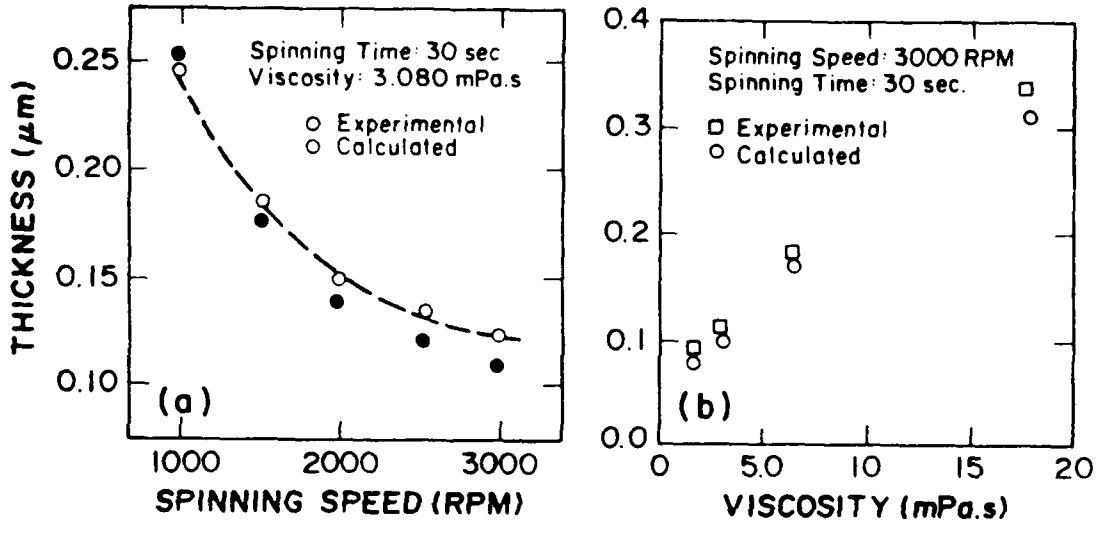

Figure 1. The calculated and experimental layer thickness of $PbTiO_3$ films as a function of (a) spinning speed at fixed spinning time and viscosity and (b) viscosity at fixed spinning time and speed.

agrees very well with the experimental values. With increasing spinning speed the shift of the values calculated by Eq. 5 from the experimental results was larger, and at a speed of 3,000 rpm the discrepancy reached 30%. This may indicate that the assumption of Newtonian behavior of the solution at high shear stress (high spinning speed) is not a good one. The calculated and experimental results of the change of fired film thickness with solution viscosity at fixed spinning speed and time are shown in Fig. 1b. At all points in Fig. 1b, the film thickness calculated from Eq. 5 is less than the experimental value, which may be due to some solvent evaporation; both C and η will increase with evaporation of the xylene solvent, and this will tend to increase the fired film thickness over that calculated by Eq. 5. However, the agreement between the predictions of Eq. 5 and the experimental results shown in Fig. 1 is reasonably good, and Eq. 5 has proven to be very useful for predicting thickness of the fired MOD films.

2.2 Pyrolysis

After deposition of the formulation solution onto a substrate, the next step in MOD processing is to increase the temperature so as to remove any remaining solvent that had not evaporated during the deposition step and to convert the metallo-organic compounds into an inorganic film. The pyrolysis must always be carried out under temperature and oxygen partial pressure conditions that are oxidizing to carbon. In most cases, the pyrolysis step is the most critical one in all of MOD processing because this is where the initial microstructure of the film is developed. A large volume change occurs during pyrolysis and this may lead to cracks in the fired film. The volume change associated with films deposited by spin coating are invariably greater than 10, and sometimes as high as 30.

Thermogravimetric analyses can be used to determine the minimum temperature required in order to remove all of the carbon from the film, and to suggest appropriate heating rates in

different temperature ranges. Figure 2 shows a thermogram of a formulation solution to produce $PbTiO_3$ [3], and the decomposition temperature (T_d) is seen to be slightly above $300^{O}C$. Therefore, the pyrolysis step can be carried out at any temperature greater than $300^{O}C$. The rate of heating from room temperature to $T > T_d$ is always very important in producing good quality films, but unfortunately no general rules can be given. Looking at the thermogram in Fig. 2 would suggest that the heating rate should be quite low during the solvent evaporation phase below $100^{O}C$, and also that rather slow heating rates seem in order between 100 and $300^{O}C$ where the compound decompositions are occurring, and for most systems studied a slow heating rate the order of $10^{O}C$/min to the decomposition temperature is preferable. However, in the case of indium-tin oxide (ITO) films just the opposite was observed [2], and nonuniformities in the films were always present if slow heating was used. It is believed that this effect was due to a wetting phenomena because both the indium and tin 2-ethylhexanoates used in the formulation solution are very viscous liquids at room temperature. One of the requirements for an ideal metallo-organic compound for MOD processing is that it decomposes without melting, but ideal compounds cannot always be found. The viscosity of both compounds used in the ITO formulation decrease with increasing temperature until thermal decomposition initiates, and in the temperature range where the compounds are still liquids the viscosity becomes sufficiently low that they will assume their equilibrium contact angle with the substrate; in the case of SiO_2 glass substrates this required the film breaking [illegible] identical ITO film processed under the same conditions on [illegible] did not show the individual droplets, but rather showed interconnected regions of thicker ITO. Nonuniformities having still different appearances were observed for films on single crystal [illegible] substrates. Since the contact angle of a liquid on a solid surface depends on the liquid-solid and solid-vapor interfacial energies in addition to the surface tension of the liquid, different behaviors would be expected on different substrate materials. It was determined that the degree

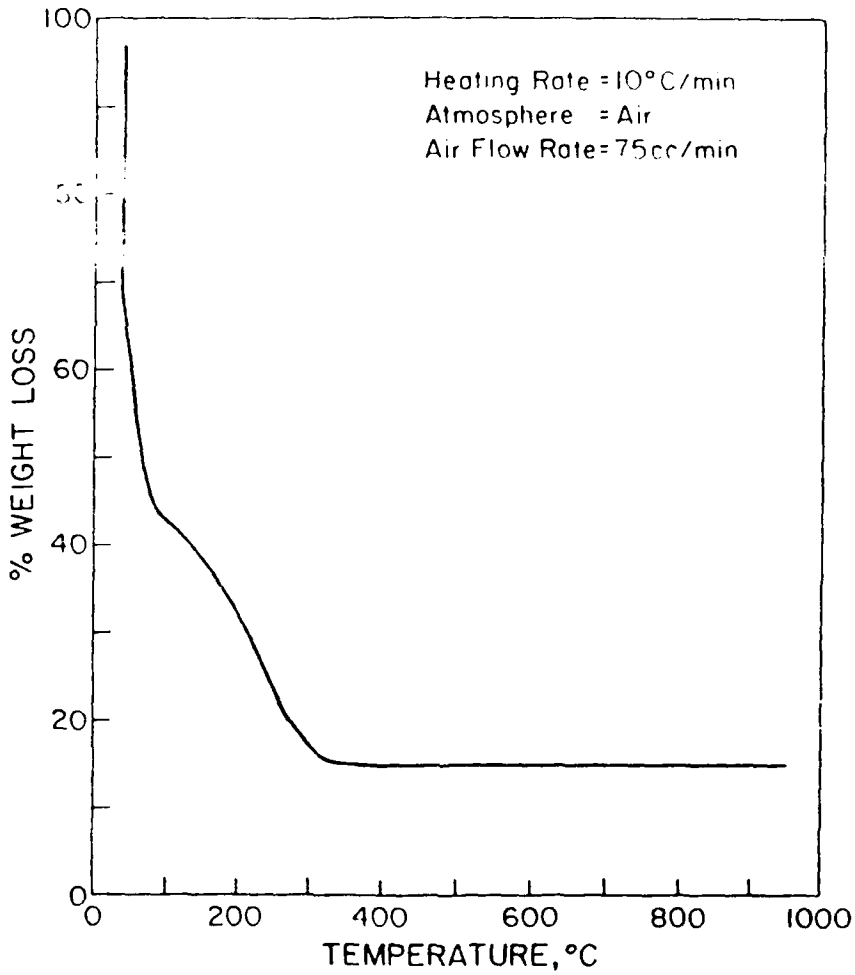

Figure 2. Thermogram of a xylene solution of an equimolar mixture of lead 2-ethylhexanoate and titanium di-methoxy-di-neodecanoate.

of nonuniformity in the ITO films decreased as the heating rate increased, and that the best quality films were obtained by inserting the substrates directly into a muffle furnace at 550°C. Using this very rapid heating rate, very uniform and transparent films were obtained. It was feared that the very rapid heating rates required to keep the films from segregating prior to decomposition would lead to rough films due to the rapid release of the organic materials. This was not the case, however, and the films fired by placing them directly into a 550°C muffle furnace had a surface roughness equivalent to that of the substrate. The direct pyrolysis was also found to be advantageous for $LiNbO_3$ films, as will be discussed in Section 5.

The thermochemistry which applies during the pyrolysis step is very complex. Figure 3 [3] is a thermogram of lead 2-ethylhexanoate which shows that T_d is about 380°C, and Fig. 4 shows a T_d of about 375°C for titanium di-methoxy-di-neodecanoate although a small additional weight loss is observed between 375° and 500°C. When these two compounds dissolved in xylene are mixed to give a $PbTiO_3$ formulation solution, the thermogram of Fig. 2 is obtained, which shows that T_d is lower than for either of the individual compounds. This result indicates that some type of "domino effect" is operative in the decomposition of a mixture of compounds.

The most likely pyrolysis mechanism for carboxylates $M(RCOO)_z$ involves a rate determining free radical generation by thermal fission, followed by a fast fragmentation of the radical [4] and a very fast oxidative chain reaction. The free radical mechanism would account for the observed "domino effect". If this is the mechanism, then the decomposition temperature should decrease as the chain length of R increases, as the oxygen partial pressure increases, and as the degree of branching of R increases. These predictions have been found to be valid in many, but not all cases. A study [5] of the decomposition temperature for five different silver carboxylates with R containing 3 to 9 carbon atoms, and with branching varying from primary to secondary to tertinary, showed that the decomposition temperatures of all compounds were

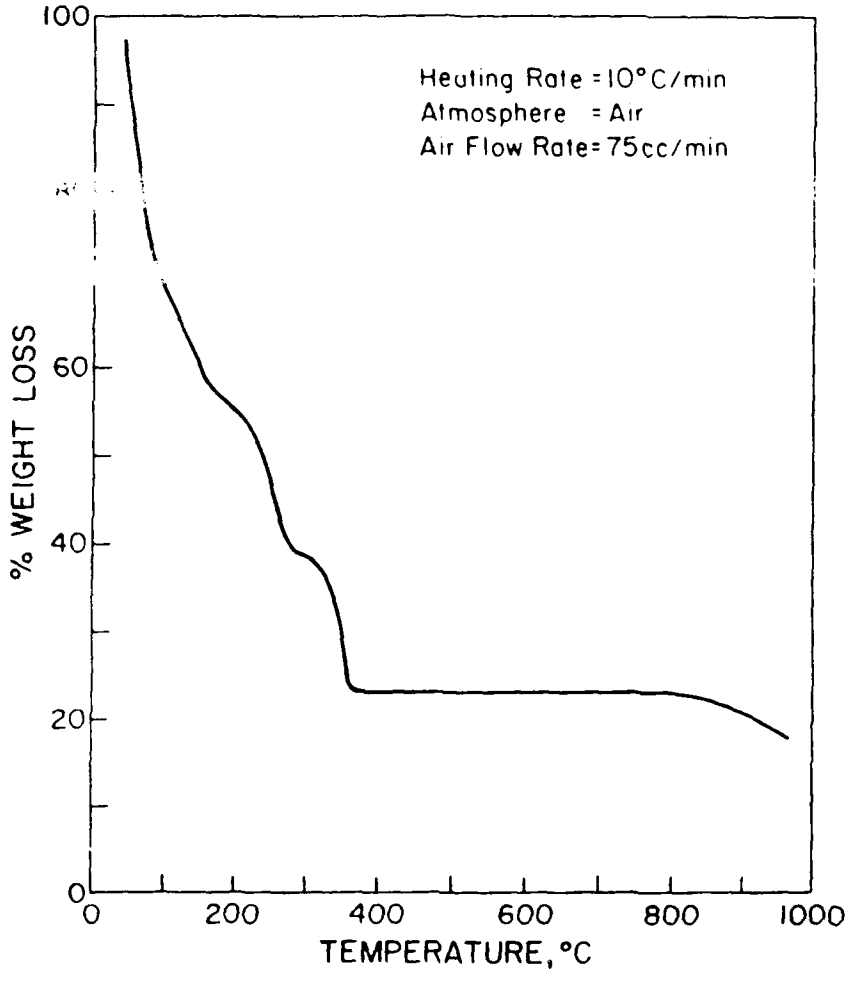

Figure 3. Thermogram of lead 2-ethylhexanoate solution in xylene.

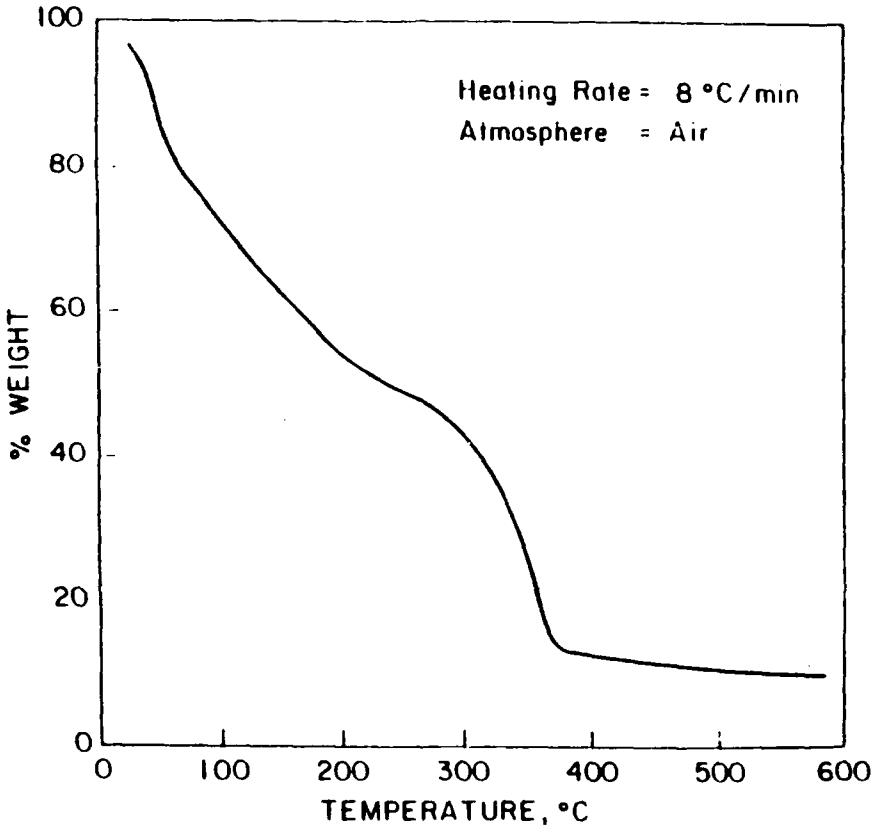

Figure 4. Thermogram of $(CH_3O)_2Ti(C_9H_{19}COO)_2$ solution in xylene.

with 5°C of each other; this result indicates that it is the silver-oxygen bond that fractures first to initiate the decomposition, and that the nature of the organic radical is immaterial in affecting the decomposition temperature. The thermochemistry involved in pyrolysis of this class of metallo-organic compounds is a fertile area for more basic research.

One of the advantages of MOD processing is illustrated by comparing Figs. 3 and 2. The decrease in weight above 800°C in Fig. 3 is due to vaporization of PbO, which is a common problem during processing of lead containing ceramics. However, when the lead 2-ethylhexanoate is mixed with titanium di-methoxy-di-neodecanoate the reactivity during pyrolysis is so high that crystalline $PbTiO_3$ is formed below 500°C [6] and no lead loss is observed at higher temperatures (Fig. 2).

2.3 Annealing

If the MOD films are fired to temperatures only slightly above the decomposition temperature during the pyrolysis they usually show an amorphous x-ray diffraction pattern, as shown in Fig. 5 for the $PbTiO_3$ film fired at 435°C for one hour [6]. Annealing at higher temperatures develops the crystallinity of the film as indicated for the 475 and 494°C anneals in Fig. 5. The increase in grain size with increased annealing temperatures can be followed by using x-ray line broadening techniques, and an example of such results [7] for $BaTiO_3$ films are shown in Fig. 6 for one hour anneals at temperatures from 780° to 1200°C. The extent of grain size control by annealing is often limited by substrate-film interactions. For example, the grain size data in Fig. 6 for temperatures of 1100°C and below were taken for films deposited on ITO coated silicon wafers. When these films were annealed at temperatures above 1100°C, the x-ray diffraction patterns showed some new peaks which were not characteristic of $BaTiO_3$, ITO or silicon, which indicated that a new phase or phases had formed due to interactions in the

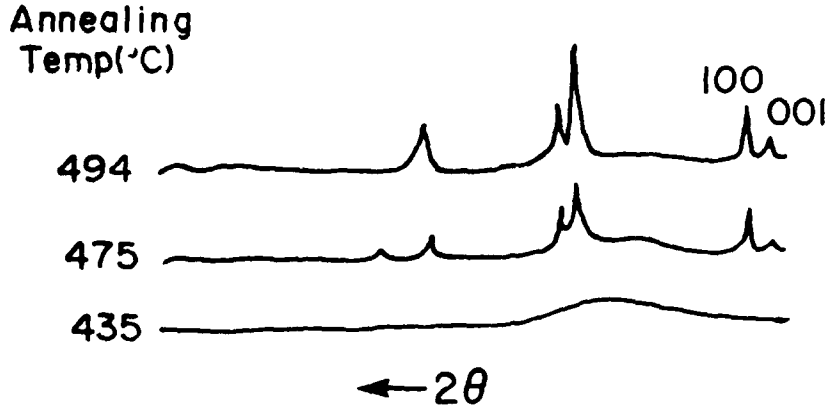

Figure 5. X-ray diffraction patterns (with CuK_α) for films (1 μm) fired on Pt foil at various temperatures.

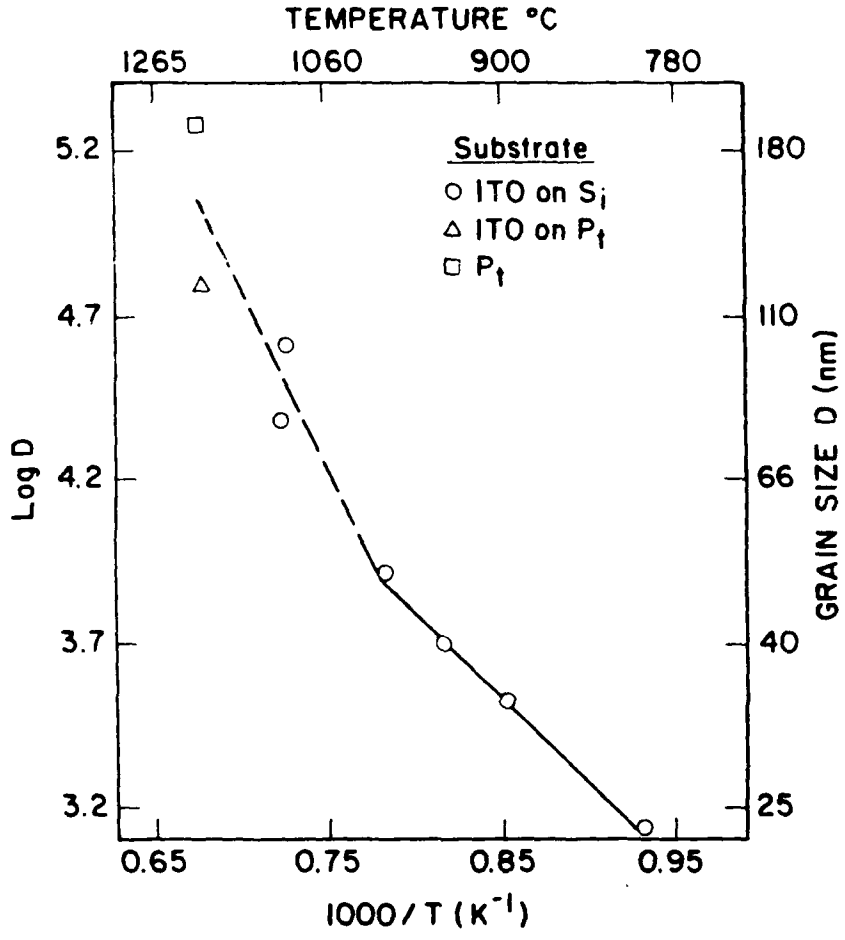

Figure 6. Grain growth kinetics for 1 hour anneal of $BaTiO_3$ films.

film-electrode-substrate system.

While MOD films are always polycrystalline, it is sometimes possible to achieve preferred orientation during the annealing step. The x-ray diffraction pattern in Fig. 7 [3] for a MOD platinum film on a (111) silicon substrate shows a very strong degree of (111) preferred orientation, which is probably due to an epitaxial effect. Figure 8 [3] shows x-ray diffraction patterns for PLZT, $Pb_{0.92}La_{0.08}(Zr_{0.65}Ti_{0.35})_{0.98}O_3$, films on (1010) sapphire substrates annealed at two different temperatures compared to the x-ray diffraction pattern of powder having the same composition. The pattern of the film annealed at 650^{o}C was identical to the power pattern, indicating random orientation of the grains in the film, but the pattern of the film annealed at 750^{o}C shows that the grains were oriented with (001) planes parallel to the substrate surface. This preferred orientation cannot be due to an epitaxial effect because there is a large lattice mismatch between (1010) sapphire and (001) PLZT.

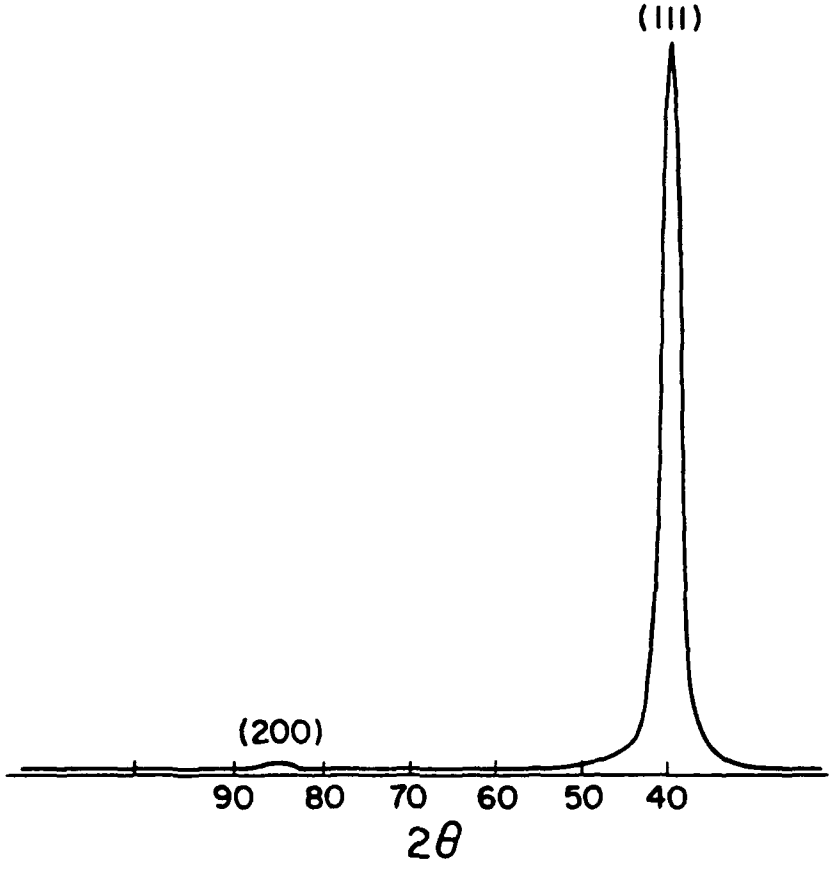

Figure 7. X-ray diffraction pattern of thin (60 nm) MOD Pt film on (111) Si wafer.

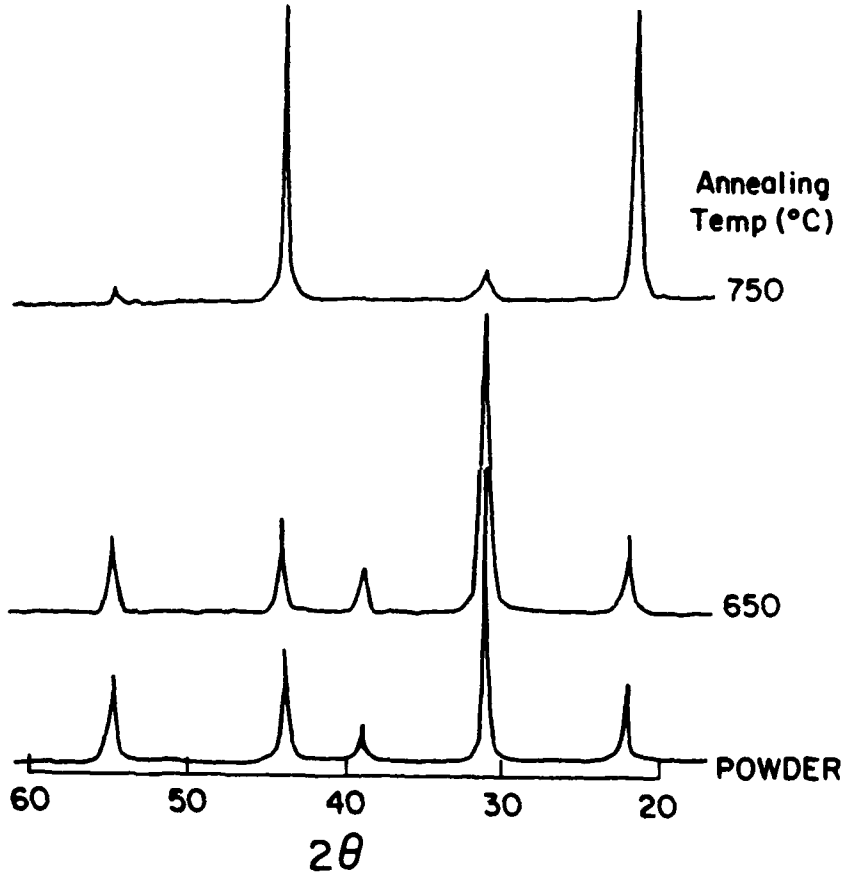

Figure 8. Comparison of x-ray diffraction patterns of PLZT films annealed at 750°C on (1010) sapphire with powder of the same composition.

3. PZT FILMS

The potential applications of ferroelectrics for the nonvolatile storage of information have long been recognized because the polarization state can correspond to binary digital information. However, the direct application of a ferroelectric capacitor as a memory cell requires a near square loop configuration with a well defined coercive field, which led to research on materials such as KNO_3. The more recent approach to ferroelectric memories has been to integrate the ferroelectric memory capacitor into a random access memory (RAM) circuit, in which the capacitors are only activated to store data upon loss of powder and restore data upon regaining power. In this way the current RAMs can be converted to a nonvolatile form while maintaining the same monolithic architecture simply by adding the ferroelectric capacitor to the top of the chip. This application requires that the ferroelectric be present in thin film form, and the film must be very uniform over the surface of the integrated circuit so that the ferroelectric capacitor associated with each memory cell is the same. One of the advantages of MOD processing of ferroelectric films is the ability to achieve uniform films over large areas as demonstrated with our results on lead titanate [6]. The materials of choice for the ferroelectric memory capacitors at the present time are PZT or PLZT. Given our success in preparing films of PT [6] and PLZT [1] by the MOD process, it was decided to undertake a feasibility study of producing PZT films suitable for memory applications.

It was decided to use the same precursor compounds as were successful for preparing PLZT, as described in the previous annual report [1]. These compounds were: lead 2-ethylhexanoate ($Pb(C_7H_{15}COO)_2$), zirconium n-propoxide ($Zr(OC_3H_{7)_4}$), and titanium di-methoxy-di-neodecanoate ($((CH_3O)_2Ti(C_9H_{19}COO)_2$). The composition chosen was $PbZr_{0.2}$ $Ti_{0.8}$ O_3. Figure 9 shows a thermogram for the PZT formulation solution with xylene solvent. The formulation solution was completely converted to PZT by 330^{o}C and produced

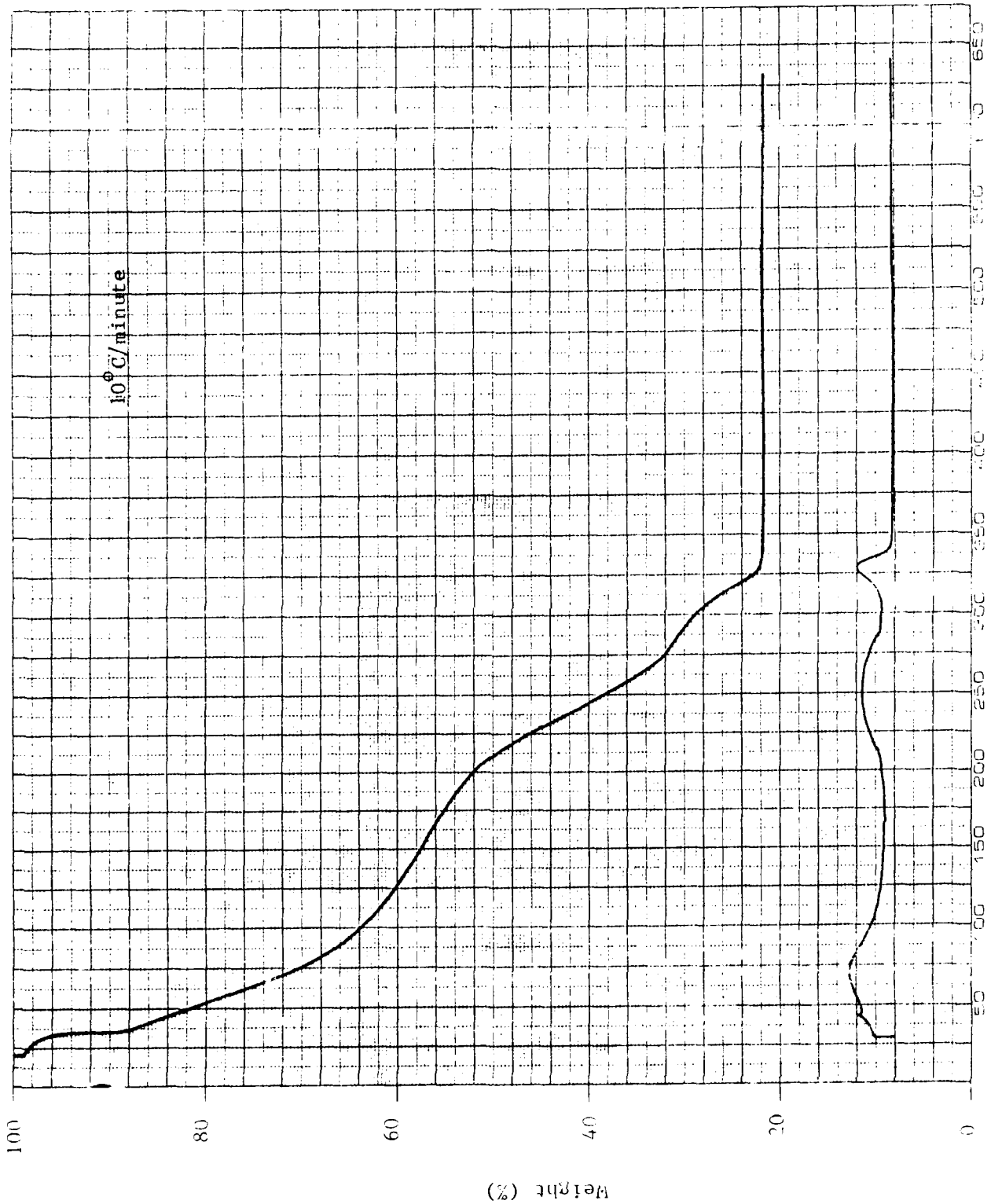

Figure 9. Thermogram of PZT formulation solution.

approximately 22 wt.% of the inorganic phase. The substrate selected was silicon wafers with 10-20 nm evaporated Ti plus approximately 300 nm evaporated Pt. The formulation solution was deposited on the substrate by spinning at 1500 rpm for 30 seconds. The wet films were then fired using a variety of heating rates and maximum temperatures. Capacitors for tests were prepared by sputtering a Pt top electrode followed by annealing at 750^{O}C in oxygen.

In order to be useful as memory capacitors, the PZT film must be crack free and pin hole free. The cracking of the films is related to both the wet film thickness and the heating rates used to the pyrolysis temperature. Preliminary experiments showed that almost any heating rate could be used if the concentration of precursor compounds in the formulation solution was reduced to a point that 16 wt.% or less of PZT was formed on thermal decomposition.

Our previous work with PT [6] found that a metastable pyrochlore phase formed under certain processing conditions, and this was also found to be a problem with the PZT films. Figure 10 shows x-ray diffraction patterns of single layer (160 nm thick) films fired at temperatures from 400 to 485^{O}C compared to a powder having the same composition. The indicated peaks in Fig. 10 are due to the pyrochlore phase. However, it was determined that all peaks corresponding to the pyrochlore phase disappeared from the x-ray diffraction pattern if the films were annealed for 5 hours at 450^{O}C. Heating the films to 465^{O}C in 15 min. or less followed by annealing for 10 hours also produced films with no indication of the metastable pyrochlore structure.

The circuit shown schematically in Fig. 11 was used to evaluate the switching characteristics of the films. This circuit is similar to one described by Camlibel [8]. A voltage pulse to produce an electric field E_f across the film, a value in excess of the coercive field, was applied to the film capacitor (C_f) in series with a reference capacitor (C_o), and the voltage (V_o) across the reference capacitor film was measured with an oscilloscope. The voltage pulses were

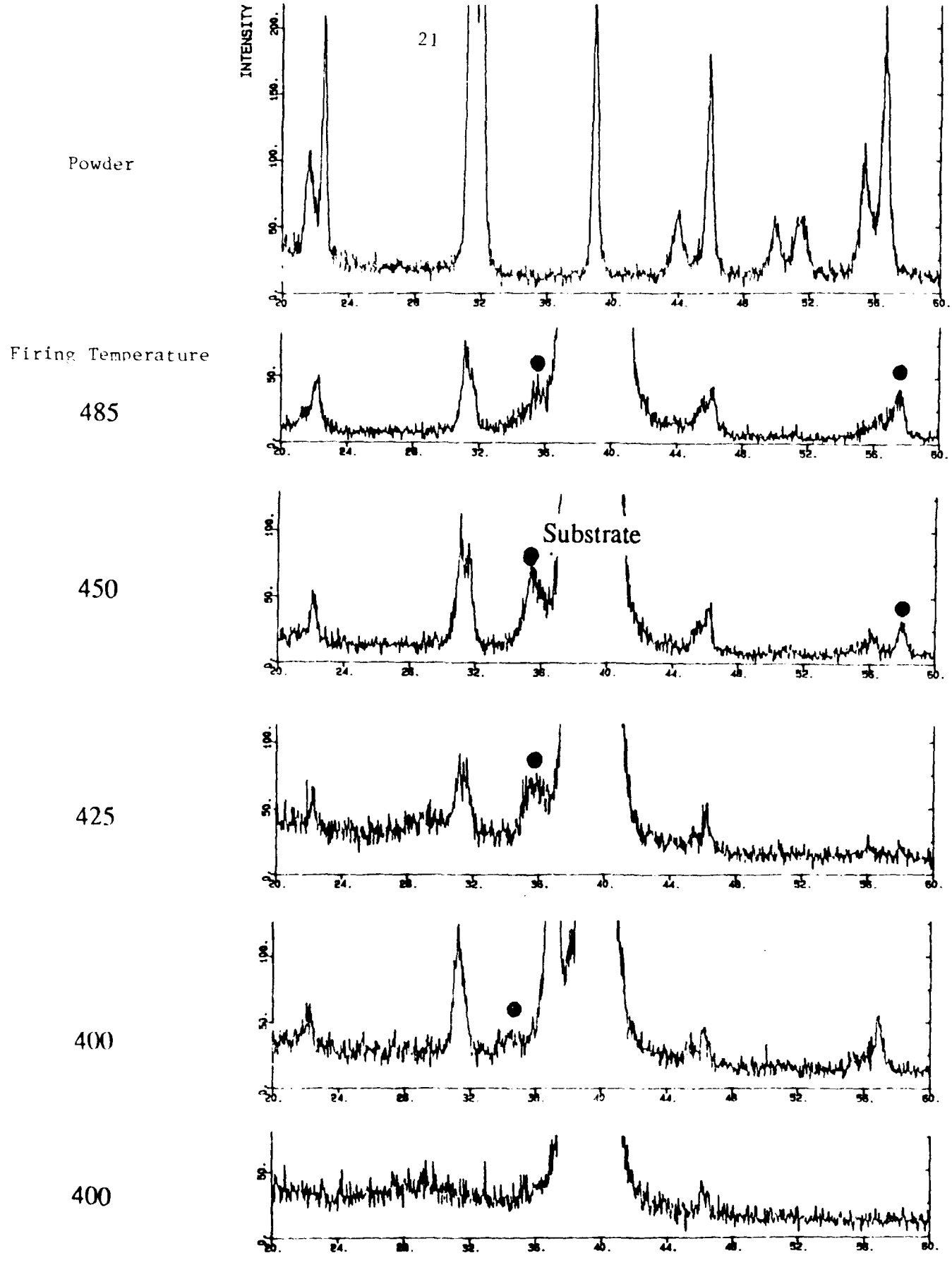

Figure 10. X-ray diffraction pattern for films 0.16 μm thick fired on Pt-Si foil at various temperature. The indicated peaks are not characteristic of tetragonal PZT.

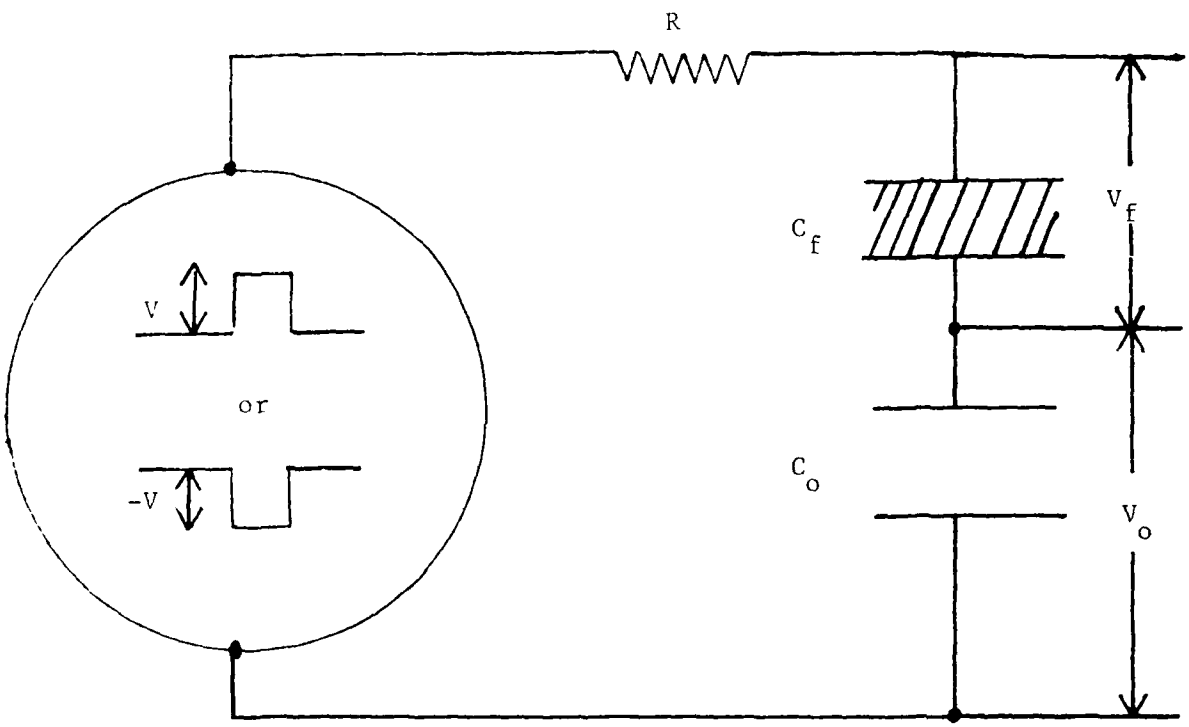

Figure 11. Circuit for evaluating switching characteristics of ferroelectric capacitors.

± 5 volts so as to be compatible with silicon technology. Typical values for the pulse duration and the time between pulses were 1 μs and 50 μs, respectively. If the film was in the negative polarization state a positive pulse would switch it to the positive polarization state, whereas if the film was in the positive polarization state a positive pulse would produce charge representative of the linear polarization only. The same considerations apply for a negative pulse. The pulse experiments can be related to the change in polarization state depicted on the idealized hysteresis loop shown in Fig. 12. In the absence of a pulse, the ferroelectric film is in polarization state P_2 or P_3, depending on the polarity of the most recent pulse. In a typical experiment, a negative pulse was applied to set the film in polarization state P_3. This was followed by two positive pulses, the first of which switched the film from P_3 to P_1 while the second switched the film from P_2 to P_1. Then two negative pulses were applied to switch the film first from P_2 to P_4 then from P_3 to P_4. The results of these experiments are given in Table 1.

Table 1. Results of voltage pulse experiments.

Switching Mode	V_0C_0 (nC)
$P_3 \rightarrow P_1$	5.44
$P_2 \rightarrow P_1$	1.42
$P_2 \rightarrow P_4$	5.47
$P_3 \rightarrow P_4$	1.69

Ideally, the same charge should be transferred when switching P_3 to P_1 as P_2 to P_1, and P_2 to P_4 or P_3 to P_4. The switching modes listed in Table 1 are typical of the small electrode polarization. The average charge transferred during polarization reversal was 5.46 nC, and that during a pulse with the same polarity as the capacitor polarization was 1.56 nC. This latter value corresponds to the charge transferred during a sensing pulse which would be used to determine if a cell is in a given polarization state. The ratio of switched charge to sensed charge for the PZT film was 5.46/1.56 = 3.5, which is sufficiently high for memory applications.

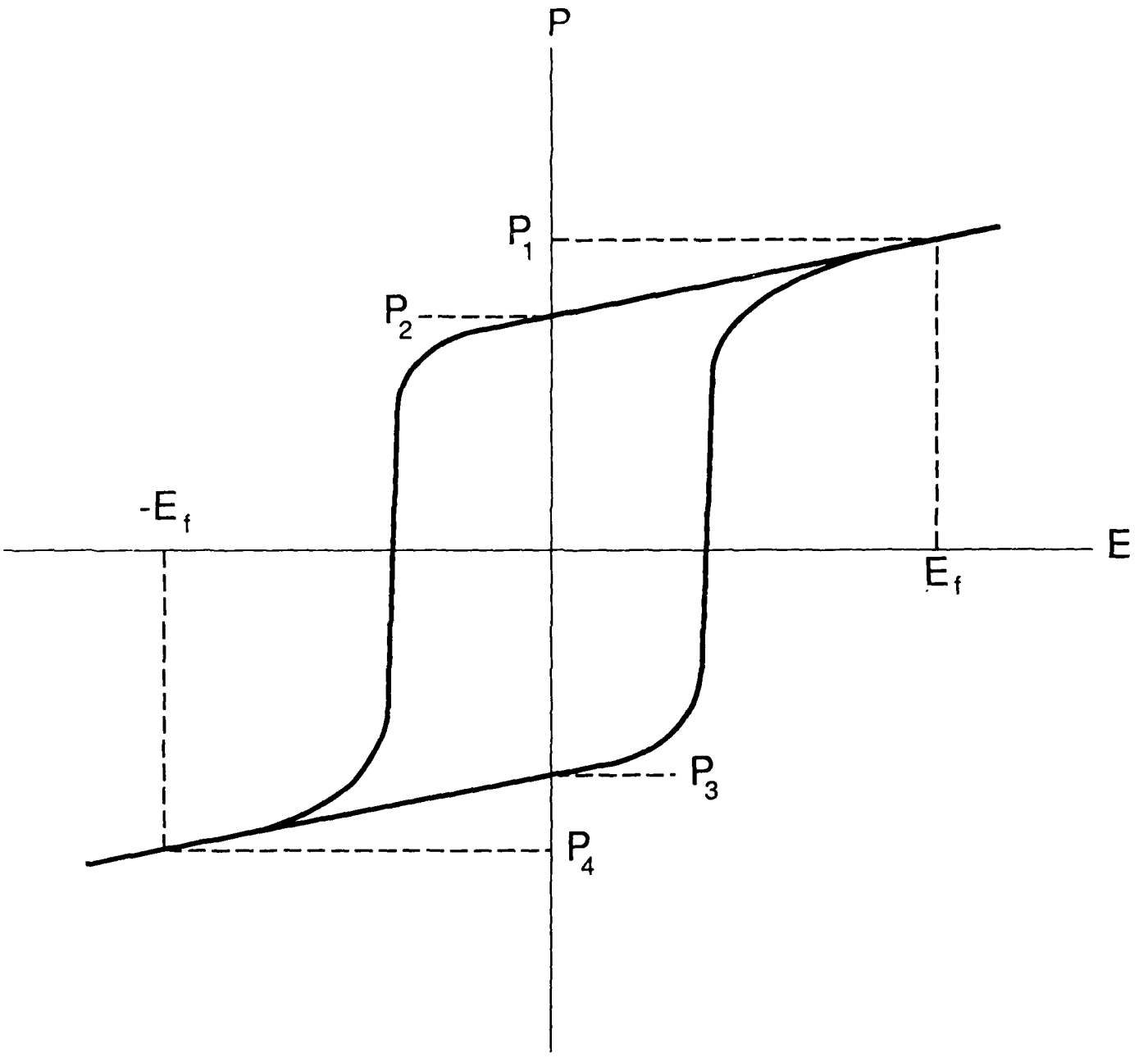

Figure 12. Polarization states during pulse experiments.

The results of the pulse experiments were analyzed by first writing the polarization as the sum of the linear plus spontaneous terms:

$$P = P_{lin} + P_s = (K-1)\,\varepsilon_o E + P_s \tag{6}$$

where K is the dielectric constant, ε_o is the permittivity of vacuum, and E is the electric field. The charge (Q) stored in the film capacitor during a switching pulse is given by

$$Q = DA = A[\varepsilon_o E + P] = A[\varepsilon_o E + \varepsilon_o E(K-1) + 2P_s] \tag{7}$$

$$Q = A(\varepsilon_o KE + 2P_s) = A(\varepsilon_o KV_f/d + 2P_s) \tag{8}$$

where D is the dielectric displacement, A is the cross-sectional area of the film capacitor and d is its thickness. The spontaneous polarization is multiplied by 2 in Eqs. 7 and 8 because the experiment calls for switching from $-P_s$ to $+P_s+P_{lin}$ or from $+P_s$ to $-P_s+P_{lin}$. The charge on either capacitor in Fig. 11.1, C_oV_o, in Eq. 8 can be expressed as

$$C_oV_o/A = \varepsilon_o KV_f/d + 2P_s \tag{9}$$

Knowing C_oV_o (Table 1) and A (10^4 μm^2) the average of the total switched polarization for both positive and negative switches was calculated to be 54.6 $\mu C/cm^2$. If a pulse is applied with the same polarity as the capacitor polarization, then Eq. 9 reduces to:

$$V_oC_o/A = \varepsilon_o KV_f/d. \tag{10}$$

The [illegible] capacitor in [illegible] polarization [illegible] 36 $\mu C/cm^2$ for a KV/d. The spontaneous polarization can be calculated simply as the difference between the [illegible] divided by 2, which gives 19.5 $\mu C/cm^2$. This is a reasonable value of spontaneous polarization for PZT.

Overall, the results of this feasibility study were quite encouraging. Films with good

switching characteristics were produced and the MOD processing employed is much simplier than sputtered films or sol-gel films. Of course, there are may other questions that must be answered before the vitality of MOD films for ferroelectric memory applications can be established. These include questions of retention, fatigue, aging, etc.

4. RELAXOR FILMS

4.1 Background

The lead-based ferroelectric relaxors have the general formula $Pb(M_1,M_2)O_3$ where M_1 is typically a low valence cation, e.g., Mg^{+2}, Zn^{+2}, Fe^{+3}, or Ni^{+2}, and M_2 is a high valence cation, e.g., Nb^{+5}, Ta^{+5} or W^{+6}. The earliest and best known lead-based relaxor, $Pb(Mg_{1/2}Nb_{2/3})O_3$ (PMN), was first synthesized by Smolenski and Bokov [9,10]. These relaxors have the perovskite structure with the large cations on the corners of the cell, the anions in the centers of the faces, and the smaller cations in the body-centered position

Studies of the dielectric properties of PMN as well as other relaxors in this group have shown that these compounds exhibit a broad maximum in the dielectric constant as a function of temperature due to a diffuse phase transition, which is different from the sharp maximum for more common ferroelectrics such as $BaTiO_2$. The properties [11] of relaxor ferroelectrics such as very high dielectric constants (up to 30,000) and broad dielectric maxima have made them promising candidate materials for capacitor dielectrics, and their large electrostrictive [12] and electro-optic [13] effects make then interesting candidate materials for other device applications. However, relaxors are extremely difficult to process without producing a stable pyrochlore phase, which will degrade the dielectric properties of the relaxors. Two major factors which make it difficult to form single perovskite phase relaxor ferroelectrics have been identified. These are the sluggish solid state reaction among the ingredient oxides at low temperatures and the loss of PbO by evaporation at high temperatures. The metallo-organic decomposition process was investigated for processing the lead-based relaxors because the high reactivity achieved at low firing temperatures insures that stoichiometry can be controlled to a greater extent than in conventional powder processing. Thus, it was anticipated that the

conditions should be more favorable towards the formation of the perovskite phase. This anticipation was based mainly on the results of our previous study of *MOD processing of* $PbTiO_3$ *films* [6], which demonstrate that the pyrochlore phase could be completely avoided in this system by the proper selection of processing conditions.

The results presented in last years annual report [1] indicated that the relative amounts of perovskite and pyrochlore phases formed depended on at least nine variables;

1. The type of metallo-organic compounds used;
2. The solvent system used;
3. The concentration of metallo-organic compounds used in the formulation solution;
4. The type of substrate used;
5. The type of electrodes used;
6. The number of layers of films deposited;
7. The time-temperature profile during firing;
8. The maximum firing temperature; and
9. The atmosphere during firing.

Studies [1] showed that suitable precursor compounds for the individual elements to form PMN, $Pb(Ni_{1/3}Nb_{2/3})O_3$ (PNN), or $Pb(Fe_{1/2}Nb_{1/2})O_3$ (PFN) were lead neodecanoate, $Pb(C_9H_{19}COO)_2$, magnesium neodecanoate, $Mg(C_9H_{19}COO)_2$, iron neodecanoate, $Fe(C_9H_{19}COO)_3$, nickel neodecanoate, $Ni(C_9H_{19}COO)_2$ and niobium tri-methoxy-di-neodecanoate, $Nb(OCH_3)_3(C_9H_{19}COO)_2$. Synthesis procedures for these compounds were described in [1]. The only one of these precursor compounds which presented any particular problem was the magnesium neodecanoate, which was found to react with moisture in the air to

form a precipitate of magnesium hydroxide. It was necessary to synthesize and store magnesium neodecanoate under moisture free conditions. The solvent system used can influence the phases formed if the metallo-organic compounds have significantly different solubilities. This can lead to segregation prior to pyrolysis, which may favor formation of the pyrochlore phase. The studies narrowed the choice of solvent to xylene or tetrahydrofuran (THF), and there was insignificant difference between the solvency of these two. However, the higher volatility of THF resulted in undesirable changes in the concentration and viscosity of the formulation solutions during processing, so xylene was selected as the solvent for formulations to be deposited by spinning. It was determined that the solubility of the metallo-organic compounds in xylene was such that the maximum amount of PMN produced upon decomposition of the saturated formulation solution was approximately 16 wt%. Formulations with concentrations near this limit are undesirable because evaporation of solvent leads to precipitation of the compounds with the lowest solubility, and hence changes the stoichiometry of the solution. It was determined that formulation solutions of a concentration to produce approximately 11 wt% of PMN were stable over extended periods of time, and this was considered to be a suitable concentration to eliminate this factor as a variable in influencing the relative amounts of pyrochlore and perovskite phases produced after thermal processing.

Studies using heating rates that varied from 1°C/min. to ~ 500°C/min. showed that this variable had no influence on the amount of pyrochlore and perovskite structures produced. Of course, the heating rate can influence film quality. The effect of the number of layers of film on the phases formed was studied by depositing up to 25 layers, each 0.1 - 0.2 μm thick. The amount of perovskite phase present in the films was found to increase as the number of layers was increased from 1 to 10, but additional layers did not change the phase composition for fixed firing temperature and atmosphere. Therefore, all subsequent studies of phase formation were conducted using films with 10 or more layers.

4.2 Experimental Procedures

4.2.1 Processing and Characterization of MO Compounds and Formulation Solutions

Neodecanoic acid was the organic acid selected for synthesizing the MO compounds. When 2-ethylhexanoic acid was used, there was some precipitation noted in the magnesium and niobium metallo-organic solutions. Both 2-ethylhexanoic and neodecanoic acids have been utilized in synthesizing the lead metallo-organic precursors. However, better mixing was observed with the other MO precursors when the neodecanoic acid was used in producing the lead metallo-organic solution. Thermogravimetric analysis (TGA) was utilized to determine the metal content of the xylene solutions of MO precursors. Table 2 lists the decomposition temperature (T_d), which is the temperature where all organics have been removed for a given heating rate, and the weight percent for each of the precursor solutions. The TGA was also used to study the thermal decomposition behavior of the formulation solutions, and these results were later utilized as guidelines in determining firing temperatures for the films. The decomposition products were identified by x-ray diffraction using Cu K_α radiation, and these results are also given in Table 2.

Table 2. Results of TGA for individual MO precursor solutions.

MOD solution	T_d (^oC)	Weight loss (%)	Resulting Compound*
Lead neodecanoate	380	12.8	PbO
Magnesium neodecanoate	420	1.8	MgO
Niobium tri-methoxy-di-neodecanoate	380	15.2	Nb_2O_5
Nickel neodecanoate	325	5.0	NiO
Iron III neodecanoate	300	4.8	Fe_2O_3

*As determined by x-ray powder diffraction

The weight loss data from the TGA plots of the individual metallo-organic solutions were

used in calculating the stoichiometric formulation solutions. After the MO precursors for the formulation solutions were mixed together, the formulation solutions were stored in a brown jar already containing molecular sieves. The TGA was performed on each of the formulation solutions and the thermograms are shown in Figs. 13-15. The decomposition temperatures were 368^{O}C for PMN, 335^{O}C for PFN, and 340^{O}C for PNN. It is interesting to note that T_d for the PMN formulation solution is lower than the T_d of all three precursor compounds. This observation is in agreement with the free radical mechanism discussed in Section 2.2.

4.2.2 Substrate and Electrode Selection

The basic requirements for the substrate and electrode materials were:

a. the linear coefficient of thermal expansion for the substrate should be a close match to the ferroelectric films;

b. there should be no detrimental reactions between the electrode, substrate and the MOD ferroelectric films; and,

c. the electrode should be smooth and have good adhesion to the substate.

The thermal expansion of PMN is unusual in that is shows almost no change in length from room temperature to 100^{O}C, an increasing strain from 100 to 300^{O}C, and a near linear change in strain with temperature from 300 to 500^{O}C [14]. The mean coefficients of linear thermal expansion calculated from the strain data are: 3.8 ppm/^{O}C from 25 to 300^{O}C; 5.1 ppm/^{O}C from 25 to 400^{O}C; and 6.2 ppm/^{O}C from 25 to 500^{O}C. Good adhesion between the relaxor films and the substrates was experimentally determined to occur in the range 450 to 550^{O}C. Therefore, the ideal thermal expansion for the substrate should be ~ 7 ppm/^{O}C so that the film will be under a slight compressive stress. The substrate materials evaluated, in order of

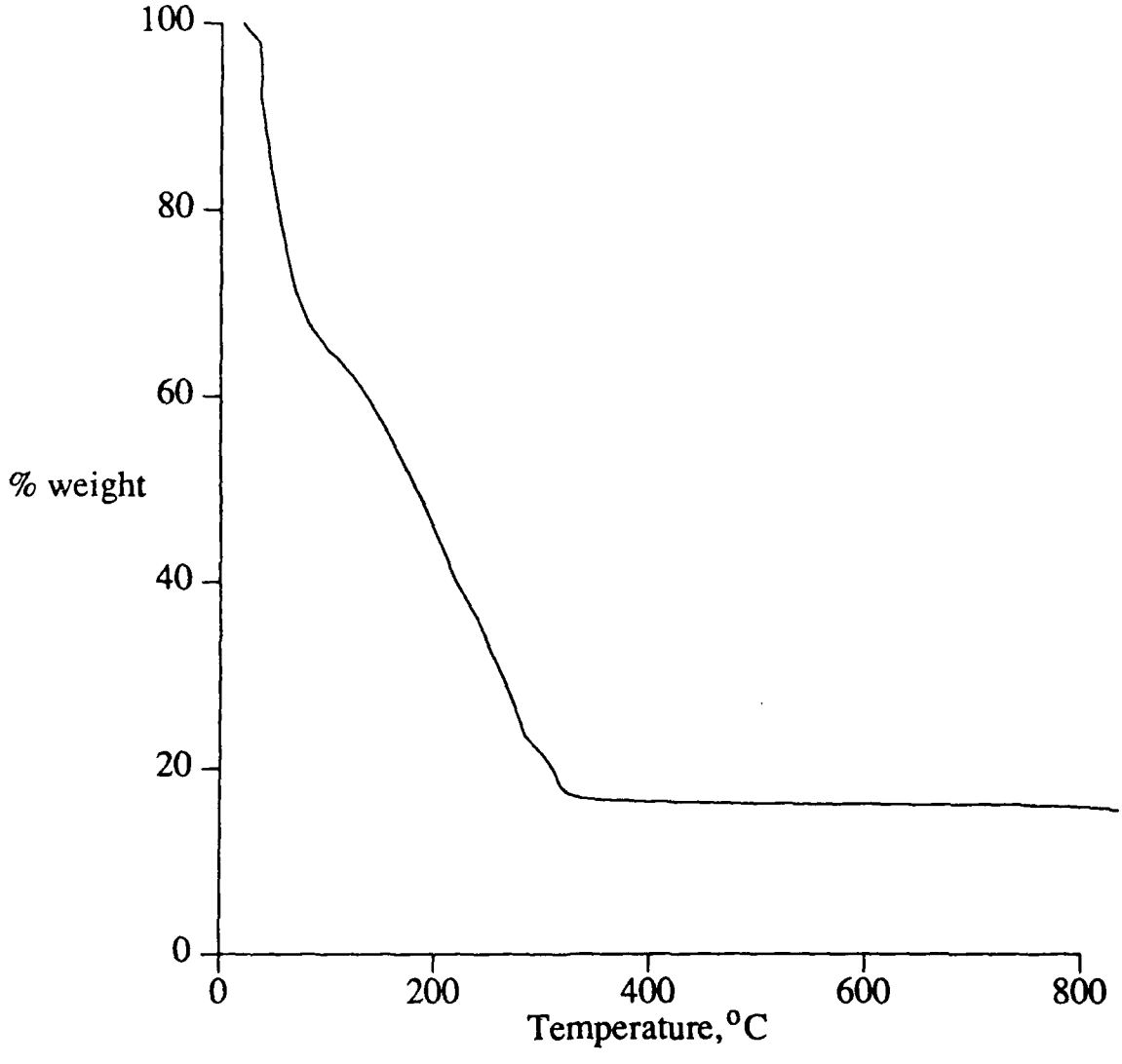

Figure 13. TGA of lead magnesium niobate solution.

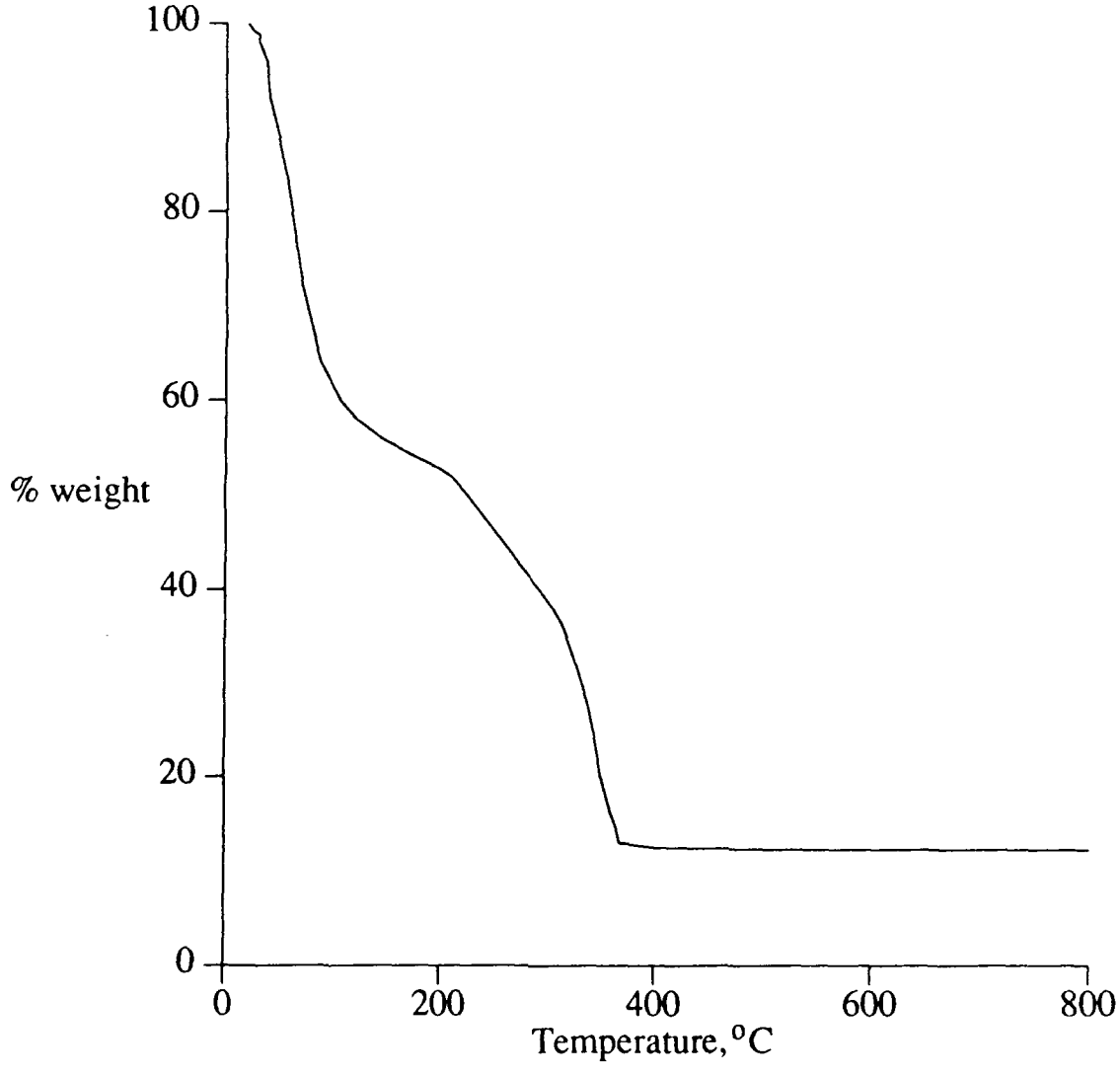

Figure 14. TGA of lead iron niobate solution.

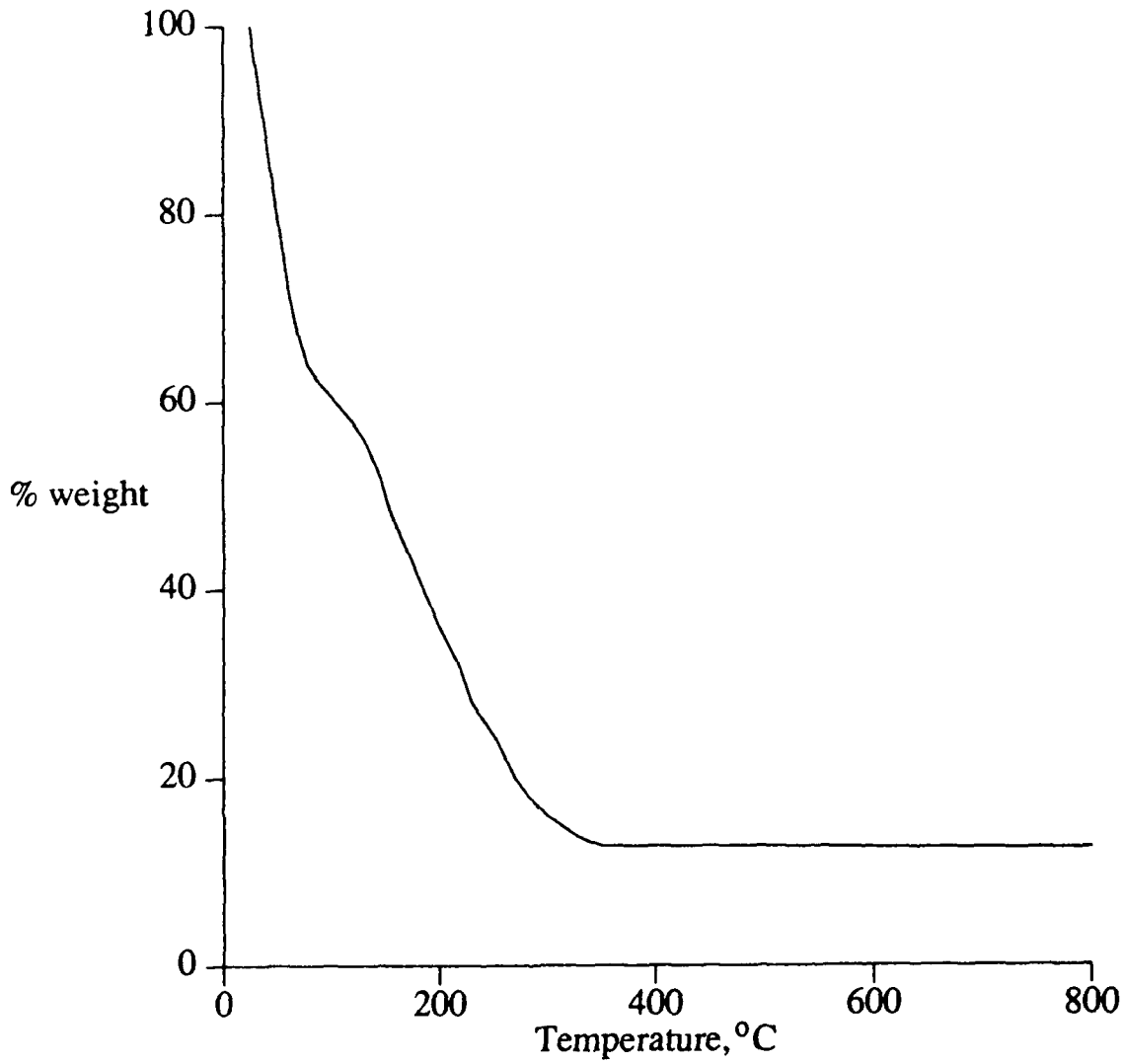

Figure 15. TGA of lead nickel niobate solution.

decreasing coefficients of thermal expansion, were platinum, sapphire, 96% alumina, silicon, cordierite, and SiO_2 glass. Of these, sapphire and alumina were closest to the ideal considering only thermal expansion matching between film and substate.

All substrate materials other than platinum had to be provided with a conducting film electrode. The electrode materials evaluated for the conducting film were platinum deposited either by sputtering or by MOD technology, gold deposited by MOD technology, and ITO (indium-tin oxide) deposited by MOD technology. It was established early in the project that Pt substrates (1.25 mm thick) were non-reactive with the MOD relaxor films, and films prepared on them were subsequently used to compare with films produced on other substrate-electrode combinations. Relaxor films prepared on the cordierite and SiO_2 glass with any of the 3 electrode films and on Si with ITO electrode film showed more pyrochlore phase compared to films processed identically on Pt substrates. It was determined that firing temperatures – 800^{o}C were required to produce relaxor films with near 100% perovskite phase; at these temperatures platinum silicides formed when Pt electrodes on Si were used, and Au diffused into the Si when gold electrodes were used. It was determined that the surface roughness of the alumina was too great to give satisfactory MOD relaxor films, but no chemical interactions were detected. In addition to platinum, the only substrate-electrode combination found to be completely non-reactive with the MOD relaxor films was MOD gold film on sapphire; all of the film studies discussed in Section 4.3 were conducted using one or the other of these two substrates.

4.2.3 Film Formation

The wet film thickness and uniformity was controlled by the concentration of the formulation solutions as well as spinning speed and spinning time. The spinning speed and time throughout the film studies were 1200 rpm and 10 seconds, and the concentrations of the

formulations were between 10 and 15 w/o. The formulations tended to precipitate if the total metal content exceeded 15 w/o. The concentrations, then, were adjusted with the addition of xylene in order to bypass the precipitation problem.

The wet films were usually dried initially at 150°C and then at 325°C in order to remove the xylene and most of the organics. Several variations in drying the films and then pyrolyzing the films were investigated.

4.2.4 Perovskite-Pyrochlore Phase Analysis

Previous studies have used a weighted fraction of peak intensities of the most intense pyrochlore and perovskite peaks observed in the x-ray diffraction analyses to determine the percent perovskite in those samples. This relation is given by:

$$\% \text{ perov} = \frac{I_{perov}}{I_{perov}+I_{pyro}} \times 100 \tag{11}$$

Equation 10 is wrong since it only gives a relative comparison of the volume fraction of the perovskite phase in the samples by using the peak height. The correct relation to account for the amount of perovskite present can be derived by using the integrated intensities of the perovskite peaks. The equation for the integrated intensity [15] is given as:

$$I = \frac{I_o A \lambda^3}{32\pi r} \frac{\mu_o^2}{16\pi^2} \frac{e^4}{m^2} \frac{1}{v^2} (|F|^2 p) \frac{(1+\cos^2(2\theta))}{((\sin^2\theta)(\cos\theta))} \frac{e^{-2M}}{2\mu} \tag{12}$$

where I is the integrated intensity per unit length of diffraction line, I_o is the intensity of the incident beam, A is the cross-sectional area of the incident beam, λ is the wavelength of incident beam, r is the radius of the diffractometer circle, μ_o is the permeability of free space, e is the charge of an electron, m is the mass of the electron, v is the volume of the unit cell, F is the structure factor, p is the multiplicity factor (the number of planes in a given family of

planes, i.e., for (111), p = 8 and for (100), p = 6), θ is the Bragg angle, e^{-2M} is the temperature factor (usually 1), and μ is the linear absorption coefficient. If K is used to represent constants associated with a given machine, and R to represent a given compound and a particular (hkl) in Eq. 12:

$$K = \frac{I_o A \lambda^3}{32\pi r} \frac{\mu_o^2}{16\pi^2} \frac{e^4}{m^2} \tag{13}$$

$$R = \frac{1}{v^2} (|F|^2 p) \frac{1+\cos^2 2\theta}{\sin^2\theta\cos\theta} e^{-2M} \tag{14}$$

The integrated intensity then simplifies to:

$$I = \frac{KR}{2\mu} \tag{15}$$

Equation 15 can be used in considering a mixture of 2 phases α and β with volume fractions V_α and V_β. Concentrating on a particular diffraction line of each phase, gives:

$$I_\alpha = KR_\alpha \frac{V_\alpha}{2\mu_m} \tag{16}$$

and

$$I_\beta = KR_\beta \frac{V_\beta}{2\mu_m} \tag{17}$$

where μ_m is the linear absorption coefficient of the mixture. Division of these equations yields:

$$\frac{I_\alpha}{I_\beta} = \frac{R_\alpha V_\alpha}{R_\beta V_\beta} \tag{18}$$

This gives a ratio of the volume fractions of the two phases.

For the case of lead based ferroelectrics, two phases are dominant, $Pb_3Nb_4O_{13}$, a cubic pyrochlore phase, and the perovskite phase, in different concentrations for a given sample. If the integrated intensity of the perovskite peak is considered for a sample containing some amount of pyrochlore and the integrated intensity of the perovskite peak for a sample containing only perovskite, Eq. 18 reduces to:

$$\frac{I_{perov(w/pyro)}}{I_{perov(w/o-pyro)}} = \frac{V_{perov(w/pyro)}\mu_{perov}}{V_{perov(w/o-pryo)}\mu_{perov+pyro}} \tag{19}$$

since $R_{perov(w/pyro)}$ and $R_{perov(w/o-pyro)}$ represent the same θ, hkl, and substance. The linear absorption coefficients can be assumed to be equal since there is only a small difference in the composition of the perovskite and pyrochlore phases. Equation 19, then, gives the volume fraction of the perovskite phase present in a sample.

Equation 19 was used in the phase analyses for the lead based relaxor MOD powders and films. X-ray diffraction using Cu K_α radiation was used to identify the phases present. The ingetrated intensities were automatically calculated by the software package for the x-ray diffractometer.

4.3 Results

4.3.1 Phases Formed in Relaxor MOD Ferroelectrics

4.3.1.1 Powders

The development of the perovskite phase in relaxor ferroelectric powders produced from the MO formulations was studied. Lead magnesium niobate was chosen for this study because of its popularity and relative ease of fabrication compared to the other relaxors. The effects of various heating rates, atmospheres and temperatures on the phases formed for PMN powder

produced from ~ 3 mg of formulation solution were determined. The samples were heated at different rates from room temperature to T_{max}, held at T_{max} for 5 minutes, then cooled to room temperature at 20°C/min. The phases were identified with X-ray diffraction using Cu K_α radiation, and the total amount of product produced was determined by weighing. Table 3 gives the results of these experiments in air and in O_2 atmospheres. The lowest temperature where perovskite PMN was identified was 700°C for the different heating rates and atmospheres. Two pyrochlore phases, $Pb_2Nb_2O_7$ and $Pb_3Nb_2O_8$, were both present for the 500°C T_{max} with the 5°C/min. heating rate in air, but $Pb_3Nb_2O_8$ was the only pyrochlore phase detected for all other conditions. Lead oxide, both litharge and massicot, was detected for several of the different heating rates and maximum temperatures. The only significant difference in the phases formed in the two atmospheres is the increased amount of PbO observed in the O_2 atmospheres.

It was noted during the x-ray analysis that no compound containing MgO was detected between 500-650°C for both air and oxygen atmospheres. Above 650°C, the perovskite PMN was identified and thus, the "missing" MgO had to be present in order to form the stoichiometric PMN. To search for the missing MgO, TEM samples were prepared by spinning the PMN formulation on NaCl substrates, 1 cm x 1 cm x 0.1 cm. Each PMN-coated NaCl substrate was dried at 150°C for 15 min., held at 325°C for 15 min., and then heated from 325°C to either 400°C or 600°C at 5°C/min. The NaCl substrates were then dissolved to give the samples used for TEM studies. For the sample fired to 500°C, the EDX analysis showed only Pb and a small amount of Nb. For the sample fired to 600°C, the EDX analysis identified Pb, Nb and Mg. The areas where Mg was dominant were small crystallites on the order of 50 nm. Electron diffraction patterns were obtained for both of the TEM samples. There were more diffraction rings and spots for the 600°C sample than the 400°C sample, indicating that there were more crystalline phases present in the 600°C sample. It was not possible, however, to identify specific phases. The TEM analysis did confirm the existence of all of the constituents necessary

Table 3. Yield and phase analysis for PMN powders.

		Air Atmosphere		O_2 Atmosphere	
T_{max} (°C)	Heating Rate (°C/min.)	Yield (wt.%)	Phases*	Yield (wt.%)	Phases*
500	5.0	14.0	$Pb_3Nb_2O_8$ $Pb_2Nb_2O_7$	-	-
	2.5	14.8	$Pb_3Nb_2O_8$ PbO	-	-
550	10.0	14.2	$Pb_3Nb_2O_8$	-	-
	5.0	14.0	$Pb_7Nb_2O_8$ PbO	-	-
	2.5	14.4	$Pb_3Nb_2O_8$ PbO	-	-
600	10.0	12.4	$Pb_3Nb_2O_8$ PbO	15.6	$Pb_3Nb_2O_8$ Pb_3O_4
	5.0	13.2	$Pb_3Nb_2O_8$ PbO	-	-
	2.5	15.2	$Pb_2Nb_2O_8$ PbO	16.0	$Pb_3Nb_2O_8$
650	10.0	12.0	$Pb_3Nb_2O_8$	15.8	$Pb_3Nb_2O_8$ PbO
	5.0	13.9	$Pb_3Nb_3O_8$ PbO	16.0	$Pb_3Nb_2O_8$ PbO
	2.5	14.0	$Pb_3Nb_2O_8$ PbO	16.0	$Pb_3Nb_2O_8$ PbO
700	10.0	13.2	PMN	14.8	PMN, PbO
	5.0	13.8	PMN, PbO	15.8	PMN, PbO
	2.5	14.2	PMN, PbO	16.2	PMN, PbO
750	10.0	12.8	PMN	14.0	PMN, PbO
	5.0	13.6	PMN, PbO	15.2	PMN, PbO
	2.5	14.0	PMN	15.2	PMN, PbO
800	10.0	12.8	PMN	14.4	PMN
	5.0	13.2	PMN	15.8	PMN
	2.5	13.9	PMN, PbO	15.8	PMN, PbO

*Identified from x-ray diffraction analysis.

in forming perovskite PMN, and demonstrated that these oxides, when fired at temperatures below 700°C, were present as particles too small to be detected by x-ray diffraction techniques.

From the data in Table 3, it can be observed that the yield increased with decreased heating rate in both atmospheres, but that the effect of heating rate was less in oxygen than in

air. The yield also increased when going from an air to an oxygen atmosphere at a fixed heating rate. Both of these observations suggest some evaporation of one or more of the metallo-organic compounds prior to thermal decomposition because, in general, the decomposition temperature decreases with decreasing heating rate and with increasing oxygen partial pressure. The presence of PbO was detected more often at the slower heating rates and in the O_2 atmosphere at the same heating rate, but there is no unambiguous interpretation of this observation. The increase in PbO detected with decreased heating rate for T_{max} of 500-650^{O}C could be interpreted as a preferential evaporation of lead neodecanoate prior to thermal decomposition. But, the increased amount of PbO detected along with PMN for decreased heating rates and in the O_2 atmosphere for the same heating rates for T_{max} of 700-800^{O}C suggests that the magnesium and niobium compounds preferentially evaporated leaving an excess of lead.

The SEM observations of the ~ 100% perovskite powder produced by heating at 5^{O}C/min. in air to a T_{max} of 800^{O}C showed a wide range of particle sizes. There were sub-micron particles that appeared to be equiaxed, and particles up to 10 μm or greater which showed a growth habit of triangular platelets. The specific surface area of that powder, as measured by BET nitrogen absorption, was 0.54 m^2/g. Using this value of the specific surface area and assuming an average value of 5 μm for the diameter of the triangular platelets, the thickness of the platelets was calculated to be 0.56 μm, which is consistent with the SEM observations. The SEM observations of the ~ 100% perovskite powder produced by heating at 10^{O}C/min. in air to a T_{max} of 700^{O}C showed particles that appeared to be sub-micron, but they were heavily agglomerated.

4.3.1.2 Films

Wet films of PMN, PFN and PNN were prepared by spinning (1200 rpm for 10 s) the formulation solutions onto the substrates. The substrates were either platinum or sapphire with MOD gold because these had been shown to be non-reactive and to not influence the phase formation, as discussed in Section 4.2.2. The wet films were dried at 150^{o}C for 10 minutes and pyrolyzed at 325^{o}C for 20 minutes and 380^{o}C for 30 minutes. A large number of different drying and pyrolysis schedules were investigated, but they produced no significant differences in the phase formation. Some differences in phase formation were noted if subsequent layers of film were deposited after complete firing of the film as opposed to depositing subsequent layers after the 380^{o}C pyrolysis step. This led to the investigation of two different processing cycles. For processing cycle A, the next layer was spun on after the 380^{o}C pyrolysis and given the same drying and pyrolysis treatment. After the tenth layer had been applied, the furnace was ramped from 380^{o}C to T_{max} at 5^{o}C/minute in either air or O_2 and either with or without PbO pellets surrounding the sample, held at T_{max} for 1 hour, and cooled to room temperature over a period of several hours. Processing cycle A produced films ~ 1 μm thick. For processing cycle B, each layer went through the same drying, pyrolysis, and firing schedule. After the 30 minutes at 380^{o}C pyrolysis step, the furnace was ramped from 380^{o}C to 800^{o}C at 5^{o}C/minute in either air or O_2 and either with or without PbO pellets surrounding the sample, held at 800^{o}C for 1 hour, and cooled to room temperature over a period of several hours. The next layer was then spun on and the complete drying, pyrolysis, and firing schedule repeated. A total of 15 layers were deposited. The only T_{max} used for processing cycle B was 800^{o}C because the results for processing cycle A showed this to be the optimum temperature for formation of the perovskite phase in all three relaxor composition. Processing cycle B produced films ~ 1.5 μm thick.

The volume percent perovskite phase in the films was determined using the method discussed in Section 4.2.4, and the results of these studies for the three relaxor compositions are summarized in Table 4.

Table 4. Perovskite and pyrochlore phases in relaxor films.

Processing Cycle A

Comp	T_{max} (^{O}C)	v/o perovskite				Pyrochlore Phase
		air	air + PbO	O_2	O_2 + PbO	
PMN	600	0	-	-	-	$Pb_3Nb_2O_8$
	700	0	-	-	-	$Pb_3Nb_2O_8$
	750	84	-	-	-	$Pb_3Nb_4O_{13}$
	800	94	70	100	84	$Pb_3Nb_4O_{13}$
	850	81	85	97	85	$Pb_3Nb_4O_{13}$
PFN	800	100	83	87	81	$Pb_3Nb_4O_{13}$
	850	65	82	70	85	$Pb_3Nb_4O_{13}$
PNN	800	0	0	20	-	$Nb_3Nb_4O_{13}$
	850	0	-	-	-	$Pb_3Nb_4O_{13}$

Processing Cycle B

PMN	800	68	79	77	82	$Pb_3Nb_4O_{13}$
PFN	800	61	-	-	69	$Pb_3Nb_4O_{13}$
PNN	800	-	55	71	77	$Pb_3Nb_4O_{13}$

No perovskite and the pyrochlore $Pb_3NB_2O_8$ were detected in PMN films fired in air to T_{max} of 600^{O}C, in agreement with the powder results. However, the powder results showed perovskite PMN at 700^{O}C whereas the films were still 100% $Pb_3Nb_2O_8$. The perovskite PMN was present for T_{max} of 750^{O}C along with the pyrochlore $Pb_3Nb_4O_{13}$, and this particular pyrochlore was the only one detected at higher values of T_{max} for both processing cycles and all relaxor compositions. The amount of perovskite was a maximum for T_{max} of 800^{O}C for both PMN and PFN films using processing cycle A. Going from air to O_2 atmosphere generally increased the amount of perovskite phase formed, with the exception of PFN fired to 800^{O}C using processing cycle A. The PFN result was surprising because the higher oxygen partial

pressure should stabilize the desired Fe^{+3} valence state. An atmosphere rich in PbO was investigated because it has been reported [16] that it is necessary to prevent the evaporation of PbO in order to form single phase PMN, and incorporating a PbO environment when firing at the higher temperatures was shown to minimize the PbO losses [17]. The use of PbO pellets gave mixed results. They led to an increase in the amount of perovskite phase for all cases studied using processing cycle B, but led to a decrease in the amount of perovskite phase for all cases studied using the same T_{max} (800°C) with processing cycle A. This is probably due to the fact that the films were fired to 800°C fifteen times in cycle B as opposed to once in cycle A, which made the opportunity for PbO loss much greater. However, the only two films which were 100% perovskite phase (PMN at 800°C in O_2 and PFN at 800°C in air) were fired without the PbO pellets.

It is apparent from the data in Table 4 that MOD films of PNN are more difficult to prepare as single phase perovskite compared the PMN and PFN, which is in agreement with the results obtained from the ceramic processing of powders [18]. Processing cycle B yielded much more perovskite PNN compared to processing cycle A, probably because the increased time at high temperature allowed the solid state reactions to proceed to a greater extent. Many studies with ceramic relaxor compositions have shown that forming a solid solution with lead titanate (PT) stabilizes the perovskite phase. This approach was investigated by mixing the metallo-organic precursors to produce a formulation solution that would give 93 wt.% PNN plus 7 wt.% PT. A film that was 100% perovskite PNN was produced from this formulation using processing cycle B with an O_2 atmosphere, PbO pellets, and a T_{max} of 850°C. The PT solid solution approach was also investigated for PMN, with disastrous results. A formulation to give 93 wt.% PMN plus 7 wt.% PT was processed following cycle B in air with no PbO pellets. These conditions produced pure PMN films with 68% perovskite phase (Table 4), but the PT solid solution films were only 3% perovskite phase. There is no current explanation for this

observation.

The only results given in Table 4 for T_{max} values less than 800°C are for PMN films using processing cycle A, but all three relaxor compositions and the PNN-PT solid solution produced films that were predominately pyrochlore phase for T_{max} values less than 700°C regardless of the processing cycle used.

4.3.2 Film Microstructure

The MOD films looked very good after the 380°C pyrolysis step, but all relaxor films produced in this study with a significant fraction of perovskite phase were cracked. Previous studies have shown that cracking of MOD films can be due to any one or a combination of the following parameters: thermal expansion of the substrate; heating rate to the pyrolysis temperature; concentration of the formulation solution; and number of layers deposited. All four of these variables have multiple levels, which made a complete set of experiments impossibly large. Representative values for three of the parameters were selected while the fourth was varied through its levels to produce the following results. Five different substrate materials with coefficients of linear thermal expansion from 0.7 to 9 ppm/°C were evaluated; all produced cracked films. Heating rates to the pyrolysis temperature from 1 to 500°C/min. were evaluated; all produced cracked films. Concentrations of the formulation solutions from 1 to 16 wt.% were evaluated; all produced cracked films. The number of layers of film was varied from 1 to 25; all produced cracked films.

By going to a sufficient number of layers, films without open porosity could be produced because the formulation spun on for subsequent layers fills the cracks in the earlier layers. An SEM micrograph of the surface of a 15 layer PMN film is shown in Fig. 16. There is no open porosity, but severe "mud cracking" is apparent. This microstructure suggests that the film

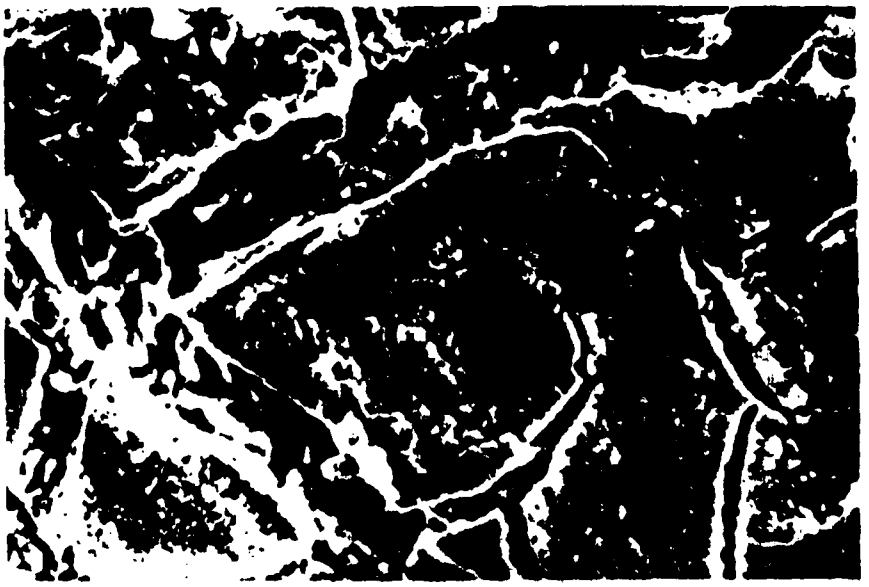

Figure 16. Cracked PMN film.

experienced extreme tensile stresses.

4.4 Discussion

The observation (Section 4.3.1.2) that all films were predominately pyrochlore phase for T_{max} values less than 700°C regardless of the processing cycle used means that the perovskite phase, which was dominant at higher values of T_{max}, formed by solid state reaction from the pyrochlore phase. This is the reaction sequence always observed during powder processing from the individual oxides, but it was hoped that the pyrochlore phase could be completely avoided due to the higher reactivity inherent with the MOD process. Such did not prove to be the case even though hundreds of different combinations of the pertinent processing parameters were used. The pyrochlore phase observed at T_{max} values of 750°C and above was $Pb_3Nb_4O_{13}$. If it is assumed that the perovskite phase forms from this pyrochlore, the solid state reaction to form PMN can be written as:

$$Pb_3Nb_4O_{13} + 3PbO + 2MgO \rightarrow 6Pb(Mg_{1/3}Nb_{2/3})O_3 \tag{20}$$

The molar volume of each of the four phases in the reaction was calculated by determining the unit cell volumes from the lattice parameters, dividing by the number of molecules per cell, and multiplying by Avogadro's number. The molar volumes were then used to calculate the relative volume change associated with the reaction with the result:

$$\frac{\Delta V}{V_i} = \frac{V_f - V_i}{V_i} = -0.116 \tag{21}$$

where V_f is the volume of 6 moles of PMN and V_i is the volume of one mole of $Pb_3Nb_4O_{13}$ plus 3 moles of PbO plus 2 moles of MgO. The surface stress (σ) produced by a fractional change in volume can be written approximately as:

$$\sigma = -K \frac{\Delta V}{V_i} \tag{22}$$

where K is the bulk modulus and the sign convention is such that a tensile stress is positive. The bulk modulus of PMN was determined to be ~ 65 GPa over the temperature range 600 to 800°C [19]. Using this value of K and the calculated relative volume change of -0.116 gives $\sigma \sim 75$ GPa (which is more than 10^6 psi). This tensile stress is well above the tensile strength of PMN, and will surely lead to failure of the films to produce crack patterns such as those shown in Fig. 16. Given the reaction sequence that cannot be avoided, crack free relaxor films cannot be produced by the MOD process.

Although the picture with relaxor films is very dim, the situation with relaxor dielectric powders by MOD processing is considerably brighter. Powders of PMN that were ~ 100 % perovskite were produced by the MOD process at temperatures as low as 700°C compared to 850°C required in conventional processing [20]. Since MOD processing does not require ball milling that must be used in conventional powder processing, a more pure powder can be produced. The PMN powders produced by firing the formulation solution in a crucible were sub-micron particle size but heavily agglomerated. By optimizing the MOD processing for powders, e.g., spray drying for pyrolysis and the 700°C conversion to perovskite phase in a fluidized bed or similar type reactor, it should be possible to produce very fine particle size powders that are not agglomerated and still maintain high purity.

5. $LiNbO_3$ FILMS

5.1 Background

Since the general concept of integrated optics was introduced [21], many theoretical and experimental studies on dielectric thin-film waveguides have been reported. As $LiNbO_3$ has excellent piezoelectric, electro-optic, and nonlinear optical properties, it is one of the most widely used materials in integrated optics for applications such as electro-optic switches, modulators, and second harmonic generators (SHG). Virtually all thin-film formation techniques have been used to prepare $LiNbO_3$ films, including liquid phase epitaxy [22,23], R.F. sputtering [24-26], chemical vapor deposition (CVD) [27], epitaxial growth by melting (EGM) [28-29], molecular beam epitaxy (MBE) [30], and sol-gel [31,32] on $LiTaO_3$, $LiNbO_3$, Si and sapphire substrates.

5.2 Experimental

The quality of the fired $LiNbO_3$ films was controlled by: (1) the choice of metallo-organic precursors; (2) the thickness of the films; (3) the rate of heating and cooling; (4) the firing temperature; and (5) the weight percent of the precursors in solution. The metallo-organic compounds used as precursors for $LiNbO_3$ were niobium tri-ethoxy-di-neodecanoate, $Nb(OC_2H_5)_3(C_9H_{19}COO)_2$, and lithium neodecanoate, $C_9H_{19}COOLi$, both in xylene solution. The compounds were synthesized following compound selection criteria and the procedures given by Vest and Singaram [33]. The synthesis reactions were as the follows:

$$Nb(OC_2H_5)_5 + 2C_9H_{19}COOH \longrightarrow 2C_2H_5OH + Nb(OC_2H_5)_3(C_9H_{19}COO)_2 \qquad (23)$$

and

$$LiOCH_3 + C_9H_{19}COOH \longrightarrow C_9H_{19}COOLi + CH_3OH \quad (24)$$

After adjusting the concentration of the compounds in xylene solution, the formulation was spun onto a substrate to make a liquid film and pyrolyzed to yield the inorganic product.

The thermal decomposition behavior of the compounds was studied using thermogravimetric analysis (TGA). From the TGA profiles, the temperatures at which the metallo-organic compounds became oxides were determined as was the weight percent of oxide produced. From these data, the weights of individual metallo-organic solutions required to form stoichiometric $LiNbO_3$ were calculated. Figure 17 shows the thermogram of $LiNbO_3$ formulation solution at a heating rate of 10°C/min. Below 150°C, the weight loss of the sample is due to evaporation of the xylene solvent. The precursor compounds begin to decompose at about 250°C and the decomposition is complete by 450°C.

A primary consideration for obtaining crack-free films is thermal expansion coefficient matching between $LiNbO_3$ and the substrate. A second important factor is the oxide weight percent of the $LiNbO_3$ precursor formulation. Sapphire was used as the substrate because of its desirable optical properties and its stability at high temperature. Although the thermal expansion coefficients are quite different between $LiNbO_3$ ($\bar{\alpha} = 13.9 \times 10^{-6}$/K) and sapphire ($\bar{\alpha} = 7.8 \times 10^{-6}$/K), crack-free thin films were made by decreasing the concentration of the metallo-organic compounds in the precursor solution to about 10% by weight for a heating rate of 20°C/min. For higher than 10% precursor solution, a lower heating rate and slower cooling rate were found to be necessary in order to minimize the crack formation. For a typical spinning rate of 1500 rpm and spinning time of 10 seconds, the single layer fired film thickness was about 120 nm; thicker films were produced by repeating the spinning and firing process.

X-ray diffraction with CuK_α radiation was used to analyze the phase composition and preferred orientation in the film, and the grain sizes were studied by SEM observation of etched

Figure 17. Thermogram of lithium niobate formulation solution.

films. Chemical etching to reveal the grain structures of $LiNbO_3$ films proved to be a problem. One part of HF and two parts of HNO_3 at the boiling point (about 110°C) for 10 minutes was reported [34] as the best etchant to reveal the domain structure of single crystal $LiNbO_3$, but this combination removed the $LiNbO_3$ films from the substrates after a few minutes. Etching experiments were conducted at room temperature for a series of etching times from 1 hour to 6 hours for different concentrations of HF and HNO_3. The result of these experiments showed that 20% of one part of HF and two parts of HNO_3 for six hours at room temperature had the best etching effect for showing grain structure in $LiNbO_3$ thin films.

5.3 Results

The x-ray diffraction patterns of the films showed $LiNbO_3$ as the only crystalline phase present for firing temperatures of 600, 700 and 800°C, and there was no evidence of a significant amount of amorphous phase. The patterns showed varying degrees of preferred orientation as evidenced by variations in relative peak intensities from those of the powder pattern, but there were no obvious correlations with firing temperature or substrate orientation.

The applications of $LiNbO_3$ thin films critically depends on good transparency, which is dependent on the light scattering characteristics. The overall scattering is determined by the porosity, grain size, and the relative refractive index and volume of any second phase present. From the x-ray diffraction results, a second phase effect can be excluded from consideration of scattering, which leaves grain size and porosity as the two major factors affecting the transparency. If the pore size is near the wavelength of the incident radiation, the light scattering will reach its maximum.

Figures 18-20 show the SEM microstructures for $LiNbO_3$ films heated at 20°C/min. from room temperature to 600°C, 700°C, and 800°C and held at the maximum temperature for 1.5

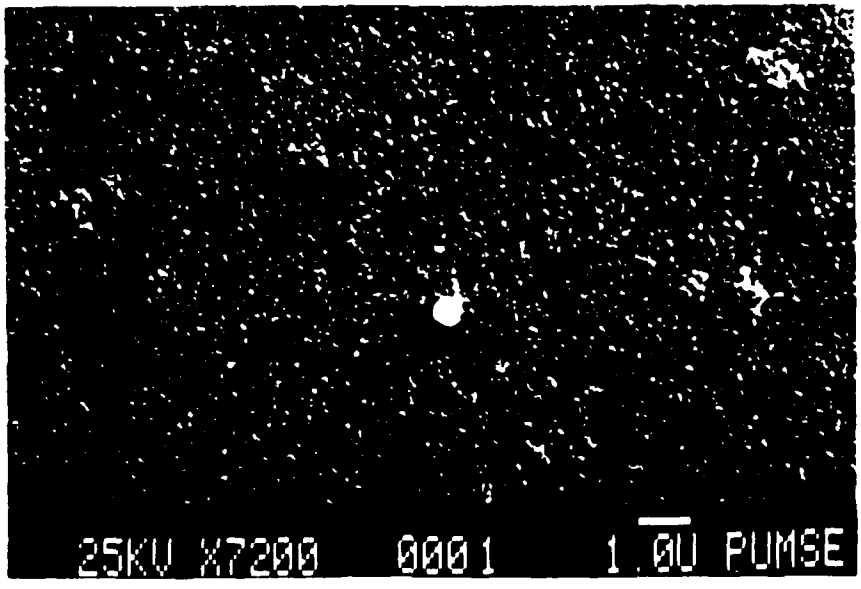

Figure 18. Etched $LiNbO_3$ film fired at $600^{o}C$ for 1.5 hours.

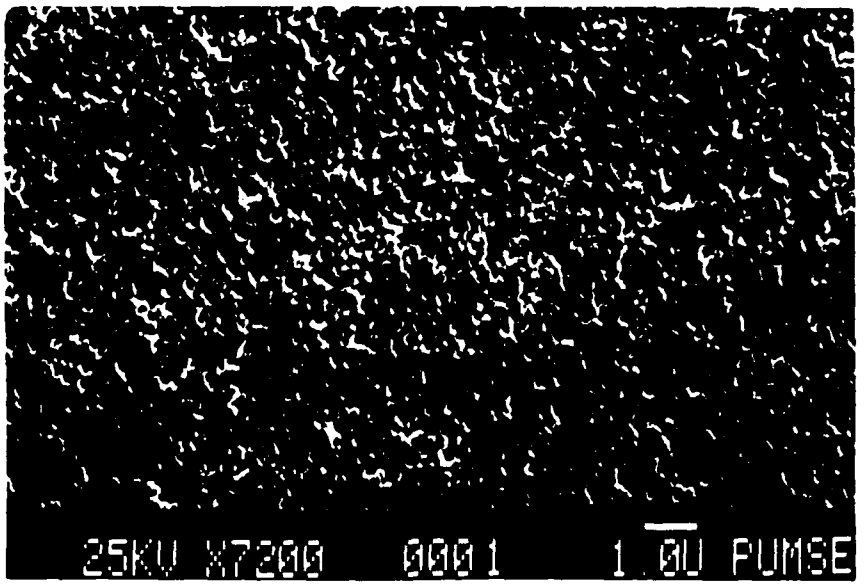

Figure 19. Etched $LiNbO_3$ film fired at 700^{o}C for 1.5 hours.

Figure 20. Etched $LiNbO_3$ film fired at 800°C for 1.5 hours.

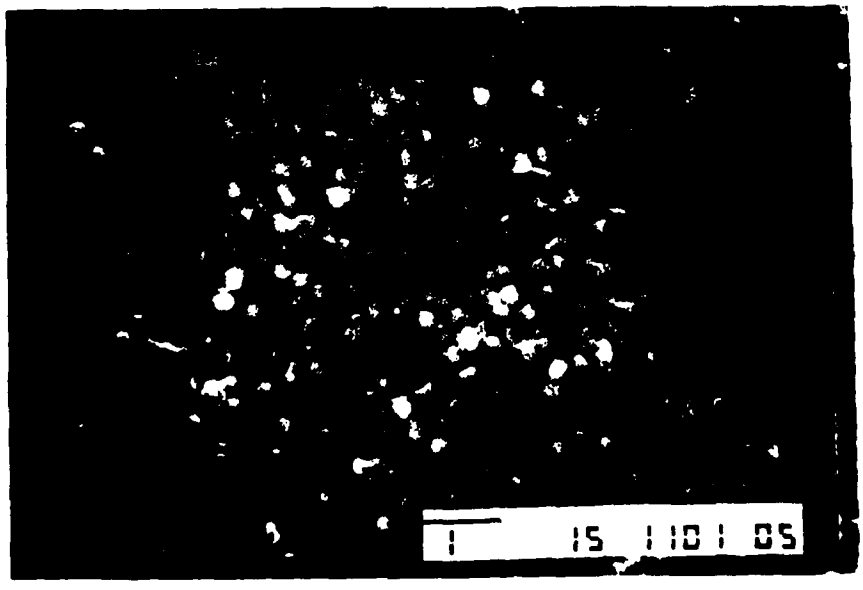

Figure 21. Etched $LiNbO_3$ film fired directly at 500°C and then heated at 800°C for 1.5 hours.

hours. For the film fired at 600°C (Fig. 18), the microstructure is very uniform and dense with grain size of approximately 85 nm, and the visual transparency was very good. For the film fired at 700°C (Fig. 19), porosity begins to develop due to grain growth (diameter = 120 nm) with preferred orientation, but the film still had good visual transparency because the average pore size was estimated to be about 150 nm. For films fired at 800°C (Fig. 20), the grain size [illegible] to 250-300 nm and the pore size and concentration also increases, leading to an opaque, white film. However, the transparency was improved by pyrolyzing the wet film directly at 500°C for 15 minutes and then heating to 800°C at 40°C/min and annealing for 1.5 hours. This rapid pyrolysis inhibits the melting of the metallo-organic compounds prior to their decomposition. Figure 21 shows that the porosity was greatly reduced and that the film microstructure was much more uniform compared to the one heated more slowly from room temperature (Fig. 20). However, while the visual transparency of this film was better than the one heated more slowly to 800°C, it was not better than that of the one fired at 700°C, probably because the grain size was 250-300 nm.

The transmittance was greater than 95% over the range 495 to 7600 nm for a film with thickness 250 nm fired at 600°C for 1.5 hours, as shown in Fig. 22. The absorption in the near UV range is dominated by electronic absorption [35]. In the infrared beginning at about 4000 nm the absorption is via the excitation of lattice vibrations. In the region between 600 and 7800 nm, the tails of both the electronic and lattice states form a local minimum in the intrinsic absorption loss. In this region the loss is dominated by scattering and probably, impurity absorption. The major difference between the bulk single crystal optical transmission [34] and the MOD film was the wider transmission window for the thin film, 253 to 8550 nm, as compared to 320 to 6200 nm. This difference is probably due to the difference in sample thicknesses; the single crystal used to measure optical transmission was 6 mm thick [34] as opposed to the MOD film 250 nm thick.

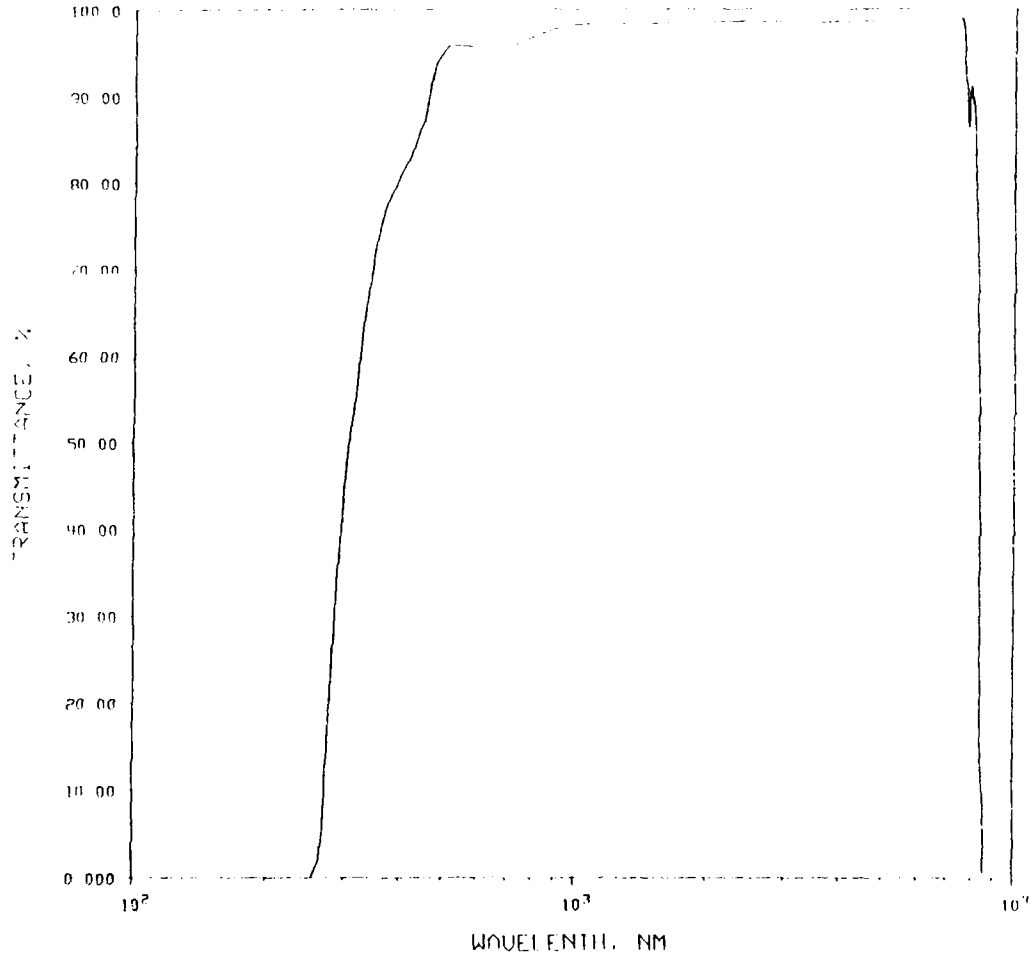

Figure 22. The transmittance of a $LiNbO_3$ film with thickness 250 nm.

5.4 Summary

1. Lithium niobate films with grain sizes 85 to 300 nm were prepared by the MOD process on sapphire substrates.

2. Films with good transparency were obtained for firing temperatures of 600 and 700°C. For films with thickness 250 nm fired at 600°C, the transmittance was greater than 95% over the range 495 to 7600 nm.

6. REFERENCES

1. R.W. Vest, G.M. Vest, A.S. Shaikh and G.L. Liedl, "Metallo-organic Decomposition Process for Dielectric Films", Annual Report for the period 4/1/87 - 3/31/88 on Contract No. N00014-83-K-0321, 15 June 1988.

2. M. Yanagisawa, Slip Effort for Thin Liquid Film on a Rotating Disc", J. Appl. Phys., 61, 1034-37 (1987).

3. J. Xu, "Preparation and Properties of Electroceramics Films using the Metallo-Organic Decomposition Process", Ph.D. Thesis, Purdue University (1988).

4. J. Xu, A.S. Shaikh and R.W. Vest, "Indium Tin Oxide Films from Metallo-Organic Precursors", Thin Solid Films, 161, 273-80 (1988).

5. G.M. Vest and R.W. Vest, "MOD Silver Metallization for Photovoltaics", Final Technical Report, 7/1/85, JPL Flat Plate Solar Array Project, Pasadena, CA, DOE/JPL-956679-84.

6. R.W. Vest and J. Xu, "$PbTiO_3$ Films from Metallo-Organic Precursors", IEEE Trans. UFFC, 35, 711-17 (1988).

7. J. Xu, A.S. Shaikh and R.W. Vest, "High K $BaTiO_3$ Films from Metallo-Organic Precursors", IEEE Trans. UFFC, 36, 307-12 (1989).

8. I. Camlibel, "Spontaneous Polarization Measurements in Several Ferroelectric Oxides Using a Pulsed - Field Method", J. Appl. Phys., 40 [4], 1690-93 (1969).

9. G.A. Smolenski, V.A. Isupov, A.I. Agranovskaya, and S.N. Popov, "Ferroelectrics with Diffuse Phase Transitions", Soviet Physics - Solid State, 2, [11], 2584-2594, (1961). Ferroelectrics, 50, 197-202 (1983).

10. V.A. Bokov, I.E. Myl'nikova, "Electrical and Optical Properties of Single Crystals of Ferroelectrics with a Diffuse Phase Transition", Soviet Physics - Solid State, 3, [3], 613-623 (1961).

11. Y. Yokomizo, T. Takahashi and S. Nomura, J. Phys. Soc. Jpn., 28, 1278-84 (1969).

12. L.E. Cross, S.J. Jang, R.E. Newnham, S. Nomura and K. Uchino, Ferroelectrics, 23, 187-192 (1980).

13. S. Nomura, H. Arima and F. Kojma, Jpn. J. Appl. Phys., 12, 531-35 (1972).

14. S.J. Jang, K. Uchino, S. Nomura and L.E. Cross, "Electrostrictive Behavior of Lead Magnesium Niobate Based Ceramic Dielectrics", Ferroelectrics, 27: 31-34 (1980).

15. D.B. Cullity, "Elements of X-ray Diffraction", Addison Wesley, Reading, MA (1962).

16. M. Inada, "Analysis of the Formation Process of Piezoelectric PCM Ceramics", Jpn. Matl. Tech. Report, 27 [1], 92-102 (1977).

17. S.L. Swartz, G.O. Dayton and D.K. Laubscher, "Low-Temperature Fired Lead Magnesium Niobate", IEEE, 2 [3], 153-156 (1986).

18. T.R. Shrout and A. Hilliyal, "Preparation of Lead-Based Ferroelectric Relaxors for Capacitors", Am. Ceram. Soc. Bull., 66 [4], 604-711 (1987).

19. G.A. Smolenski, N.K. Yushin, S.I. Smirnov, and S.N. Dorogovtsev, "Behavior of the Elastic Moduli of a Lead Magnoniobate Crystal in the Region of Coexistence of Phases", Sov. Phys. Dokl, 32 [6], 501-502 (1987).

20. W. Pan, G.O. Dayton and L.E. Cross, "Dielectric Aging Effects in Doped Lead Magnesium Niobate: Lead Titanate Relaxor Ferroelectric Ceramics", unpublished work.

21. P.K. Tein, "Light Waves in Thin Films and Integrated Optics", Applied Optics, 10 [11],

2395-2413 (1971).

22. A. Baudrant, H. Vial and J. Doval, "Liquid Phase Epitaxy of $LiNbO_3$ Thin Film for Integrated Optics", Mat. Res. Bull., 10, 1373-1378 (1975).

23. A. Baudrant, H. Vial and J. Doval, "Liquid Phase Epitaxy of $LiNbO_3$ Thin Film", J. of Crystal Growth, 43, 197-203 (1978).

24. P.R. Meek, L. Holland and P.D. Townsend, "Sputter Deposition of $LiNbO_3$ Films", Thin Solid Films, 141, 251-259 (1986).

25. G.H. Hewig, K. Jain, F.Q. Sequeda, R. Tom and Po-Wen Wang, "R.F. Sputtering of $LiNbO_3$ Thin Films", Thin Solid Films, 88, 67-74 (1982).

26. S. Takada, M. Ohnishi, H. Hayakawa and N. Mikoshiba, "Optical Waveguides of Single-crystal $LiNbO_3$ Film Deposited by RF Sputtering", Appl. Phys. Lett., 24 [10], 490-492 (1974).

27. B.J. Curtics and H.R. Brunner, "The Growth of Thin Films of Lithium Niobate by Chemical Vapor Deposition", Mat. Res. Bull., 10, 515-520 (1975).

28. Syuzo Fukunishi, Naoya Uchida, Shintaro Miyazawa and Juichi Noda, "Electro-Optic Modulation of Optical Guided Wave in $LiNbO_3$ Thin Film Fabrication by EGM Method", Appl. Phy. Lett., 24 [9], 424-426 (1974).

29. Shintaro Miyazawa, "Growth of $LiNbO_3$ Single Crystal Film for Optical Waveguides", Appl. Phy. Lett., 23 [4], 198-200 (1973).

30. R.A. Betts and C.W. Pitt, Electron. Letter, 21, 960-962 (1985).

31. I.S. Balbaa and G. Gowda, "Sol-Gel Processing of $(Na,Li)NbO_3$ System", J. Mat. Sci. Lett., 5, 751-754 (1986).

32. D.A. Barrow and J. Greggi, "Properties and Microstructure of Thin $LiNbO_3$ Films Prepared by a Sol-Gel Process", J. Mat. Res., 2 [5], 595-605 (1987).

33. G.M. Vest and S. Singaram, "Synthesis of Metallo-Organic Compounds for MOD Powders and Films", Mat. REs. Soc. Proc., 60, 35-42 (1986).

34. M. Nassau, H.J. Levinstein and G.M. Loiacono, "Ferroelectric Lithium Niobate, 1. Growth, Domain Structure, Dislocation and Etching", J. Phys. Chem. Solids, 27, 983-988 (1966).

35. Steven K. Korotky and Rodney C. Aferness, "Ti:$LiNbO_3$ Integrated Optic Technology", Integrated Optical Circuits and Components, Edited by Lynn D. Hutcheson, 169-227 (1987).